Global oceanic diazotroph database version 2 and elevated estimate of global oceanic N$_2$ fixation

Zhibo Shao[1,★], Yangchun Xu[1,★], Hua Wang[1], Weicheng Luo[1], Lice Wang[1], Yuhong Huang[1],
Nona Sheila R. Agawin[2], Ayaz Ahmed[3], Mar Benavides[4,5], Mikkel Bentzon-Tilia[6],
Ilana Berman-Frank[7], Hugo Berthelot[8], Isabelle C. Biegala[4], Mariana B. Bif[9], Antonio Bode[10],
Sophie Bonnet[4], Deborah A. Bronk[11], Mark V. Brown[12], Lisa Campbell[13], Douglas G. Capone[14],
Edward J. Carpenter[15], Nicolas Cassar[16,17], Bonnie X. Chang[18], Dreux Chappell[19], Yuh-ling Lee Chen[20],
Matthew J. Church[21], Francisco M. Cornejo-Castillo[22], Amália Maria Sacilotto Detoni[23],
Scott C. Doney[24], Cecile Dupouy[4], Marta Estrada[22], Camila Fernandez[25,26], Bieito Fernández-Castro[27],
Debany Fonseca-Batista[28], Rachel A. Foster[29], Ken Furuya[30], Nicole Garcia[4], Kanji Goto[31],
Jesús Gago[32], Mary R. Gradoville[33], M. Robert Hamersley[34], Britt A. Henke[35], Cora Hörstmann[4],
Amal Jayakumar[36], Zhibing Jiang[37], Shuh-Ji Kao[1], David M. Karl[38], Leila R. Kittu[39],
Angela N. Knapp[40], Sanjeev Kumar[41], Julie LaRoche[42], Hongbin Liu[43], Jiaxing Liu[44], Caroline Lory[45],
Carolin R. Löscher[46], Emilio Marañón[47], Lauren F. Messer[48], Matthew M. Mills[49], Wiebke Mohr[50],
Pia H. Moisander[51], Claire Mahaffey[52], Robert Moore[53], Beatriz Mouriño-Carballido[47],
Margaret R. Mulholland[54], Shin-ichiro Nakaoka[55], Joseph A. Needoba[56], Eric J. Raes[57], Eyal Rahav[58],
Teodoro Ramírez-Cárdenas[59], Christian Furbo Reeder[4], Lasse Riemann[60], Virginie Riou[61],
Julie C. Robidart[62], Vedula V. S. S. Sarma[63], Takuya Sato[64], Himanshu Saxena[41], Corday Selden[65],
Justin R. Seymour[66], Dalin Shi[1], Takuhei Shiozaki[67], Arvind Singh[41], Rachel E. Sipler[12], Jun Sun[68,69],
Koji Suzuki[70], Kazutaka Takahashi[71], Yehui Tan[44], Weiyi Tang[36], Jean-Éric Tremblay[72],
Kendra Turk-Kubo[35], Zuozhu Wen[1], Angelicque E. White[38], Samuel T. Wilson[73], Takashi Yoshida[74],
Jonathan P. Zehr[35], Run Zhang[1], Yao Zhang[1], and Ya-Wei Luo[1]

[1]State Key Laboratory of Marine Environmental Science and College of Ocean and Earth Sciences,
Xiamen University, Xiamen, Fujian, China
[2]Marine Ecology and Systematics (MarES) Research Group, University of the Balearic Islands,
Palma de Mallorca, Spain
[3]Environment and Life Science Research Centre, Kuwait Institute for Scientific Research, Salmiya, Kuwait
[4]Aix Marseille Univ, Université de Toulon, CNRS, IRD, MIO, UM 110, 13288, Marseille, France
[5]Turing Center for Living Systems, Aix-Marseille University, 13009 Marseille, France
[6]Department for Biotechnology and Biomedicine, Technical University of Denmark, Lyngby, Denmark
[7]Department of Marine Biology, Leon H. Charney School of Marine Sciences, University of Haifa, Haifa, Israel
[8]Ifremer, DYNECO, Plouzané, France
[9]Monterey Bay Aquarium Research Institute, Moss Landing, California, USA
[10]Oceanographic Center of A Coruña, Spanish Institute of Oceanography (IEO-CSIC), A Coruña, Spain
[11]Bigelow Laboratory for Ocean Sciences, East Boothbay, Maine, USA
[12]Climate Change Cluster, University of Technology Sydney, Sydney, NSW, Australia
[13]Department of Oceanography, Texas A&M University, College Station, Texas, USA
[14]Department of Biological Sciences, Marine and Environmental Biology Section,
University of Southern California, Los Angeles, California, USA
[15]College of Science and Engineering, San Francisco State University, San Francisco, California, USA
[16]Division of Earth and Ocean Sciences, Nicholas School of the Environment,
Duke University, Durham, North Carolina, USA
[17]CNRS, Université de Brest, IRD, Ifremer, LEMAR, Plouzané, France
[18]Vesta, PBC, Southampton, New York, USA

[19]College of Marine Science, University of South Florida, Tampa, Florida, USA
[20]Department of Oceanography, National Sun Yat-sen University, Kaohsiung, Taiwan
[21]Flathead Lake Biological Station, University of Montana, Polson, Montana, USA
[22]Institute of Marine Sciences (ICM-CSIC), Barcelona, Spain
[23]Institute of Marine Sciences of Andalucía (ICMAN), Consejo Superior de Investigaciones Científicas (CSIC),
Campus Río San Pedro, Puerto Real, Spain
[24]Department of Environmental Sciences, University of Virginia, Charlottesville, Virginia, USA
[25]CNRS Observatoire océanologique, Banyuls-sur-mer, France
[26]Center for Oceanographic Research COPAS Coastal, Universidad de Concepción, Vigo, Chile
[27]Ocean and Earth Science, National Oceanography Centre, University of Southampton, Southampton, UK
[28]Department of Oceanography, Dalhousie University, Halifax, Nova Scotia, Canada
[29]Department of Ecology, Environment, and Plant Sciences, Stockholm University, Stockholm, Sweden
[30]Institute of Plankton Eco-engineering, Soka University, Hachioji, Tokyo, Japan
[31]Graduate School of Environmental Science, Hokkaido University, Kita-Ku, Sapporo, Japan
[32]Spanish Institute of Oceanography (IEO-CSIC), Centro Oceanografico de Vigo, Concepción, Spain
[33]Columbia River Inter-Tribal Fish Commission, Portland, Oregon, USA
[34]Environmental Studies, Soka University of America, Aliso Viejo, California, USA
[35]Ocean Sciences Department, University of California at Santa Cruz, Santa Cruz, California, USA
[36]Department of Geosciences, Princeton University, Princeton, New Jersey, USA
[37]Second Institute of Oceanography, Ministry of Natural Resources, Hangzhou, Zhejiang, China
[38]Department of Oceanography, University of Hawai'i at Mānoa, Honolulu, Hawaii, USA
[39]Marine Biogeochemistry, GEOMAR Helmholtz Centre for Ocean Research Kiel, Düstern, Kiel, Germany
[40]Department of Earth, Ocean, & Atmospheric Science, Florida State University, Tallahassee, Florida, USA
[41]Geosciences Division, Physical Research Laboratory, Ahmedabad, India
[42]Department of Biology, Dalhousie University, Halifax, Nova Scotia, Canada
[43]Department of Ocean Science, The Hong Kong University of Science and Technology,
Hong Kong SAR, China
[44] Key Laboratory of Tropical Marine Bio-resources and Ecology, South China Sea Institute of Oceanology,
Chinese Academy of Sciences, Guangzhou, Guangdong, China
[45]French National Research Institute for Sustainable Development, IRD, Marseille, France
[46]Department of Biology, DIAS, University of Southern Denmark, Odense, Denmark
[47]Centro de Investigación Mariña da Universidade de Vigo (CIM-UVigo), Departamento de Ecoloxía e
Bioloxía Animal, Universidade de Vigo, Campus Lagoas-Marcosende, Vigo, Spain
[48]Division of Biological and Environmental Sciences, Faculty of Natural Sciences,
University of Stirling, Stirling, Scotland, UK
[49]Earth System Science, Stanford University, Stanford, California, USA
[50]Max Planck Institute for Marine Microbiology, Bremen, Germany
[51]Department of Biology, University of Massachusetts Dartmouth, Dartmouth, Massachusetts, USA
[52]Department of Earth, Ocean and Ecological Sciences, University of Liverpool, Liverpool, UK
[53]Department of Oceanography, Dalhousie University, Halifax, Nova Scotia, Canada
[54]Department of Ocean and Atmospheric Sciences, Old Dominion University, Norfolk, Virginia, USA
[55]Center for Global Environmental Research, National Institute for Environmental Studies, Tsukuba, Japan
[56]OHSU-PSU School of Public Health, Oregon Health and Science University Portland, Portland, Oregon, USA
[57]Flourishing Oceans, Minderoo Foundation, Broadway, Nedlands, WA, Australia
[58]Israel Oceanographic and Limnological Research, National Institute of Oceanography, Haifa, Israel
[59]Centro Oceanográfico de Málaga, Instituto Español de Oceanografía (IEO, CSIC), Fuengirola, Spain
[60]Department of Biology, University of Copenhagen, Helsingør, Denmark
[61]Analytical, Environmental and Geo-Chemistry & Earth System Sciences,
Vrije Universiteit Brussel, Brussels, Belgium
[62]National Oceanography Centre, Southampton, UK
[63]CSIR-National Institute of Oceanography, Regional Cente Waltair, Visakhapatnam, India
[64]Institute for Chemical Research, Kyoto University, Kyoto, Japan
[65]Department of Marine and Coastal Sciences, Rutgers University, New Brunswick New Jersey, USA
[66]Climate Change Cluster, University of Technology Sydney, Sydney, New South Wales, Australia
[67]Atmosphere and Ocean Research Institute, The University of Tokyo, Chiba, Japan

[68]Research Centre for Indian Ocean Ecosystem, Tianjin University of Science and Technology, Tianjin, China
[69]College of Marine Science and Technology, China University of Geosciences (Wuhan), Wuhan, Hubei, China
[70]Faculty of Environmental Earth Science, Hokkaido University, Sapporo, Japan
[71]Graduate School of Agricultural and Life Sciences, The University of Tokyo, Tokyo, Japan
[72]Québec-Océan and Takuvik, Department of Biology, Laval University, Québec, Canada
[73]School of Natural and Environmental Sciences, Newcastle University, Newcastle upon Tyne, UK
[74]Graduate school of Agriculture, Kyoto University, Kitashirakawa-Oiwake, Sakyo-ku, Kyoto, Japan
★These authors contributed equally to this work.

Correspondence: Ya-Wei Luo (ywluo@xmu.edu.cn)

Abstract. Marine diazotrophs convert dinitrogen (N₂) gas into bioavailable nitrogen (N), supporting life in the global ocean. In 2012, the first version of the global oceanic diazotroph database (version 1) was published. Here, we present an updated version of the database (version 2), significantly increasing the number of in situ diazotrophic measurements from 13 565 to 55 286. Data points for N₂ fixation rates, diazotrophic cell abundance, and *nifH* gene copy abundance have increased by 184 %, 86 %, and 809 %, respectively. Version 2 includes two new data sheets for the *nifH* gene copy abundance of non-cyanobacterial diazotrophs and cell-specific N₂ fixation rates. The measurements of N₂ fixation rates approximately follow a log-normal distribution in both version 1 and version 2. However, version 2 considerably extends both the left and right tails of the distribution. Consequently, when estimating global oceanic N₂ fixation rates using the geometric means of different ocean basins, version 1 and version 2 yield similar rates (43–57 versus 45–63 Tg N yr⁻¹; ranges based on one geometric standard error). In contrast, when using arithmetic means, version 2 suggests a significantly higher rate of 223 ± 30 Tg N yr⁻¹ (mean ± standard error; same hereafter) compared to version 1 (74 ± 7 Tg N yr⁻¹). Specifically, substantial rate increases are estimated for the South Pacific Ocean (88 ± 23 versus 20 ± 2 Tg N yr⁻¹), primarily driven by measurements in the southwestern subtropics, and for the North Atlantic Ocean (40 ± 9 versus 10 ± 2 Tg N yr⁻¹). Moreover, version 2 estimates the N₂ fixation rate in the Indian Ocean to be 35 ± 14 Tg N yr⁻¹, which could not be estimated using version 1 due to limited data availability. Furthermore, a comparison of N₂ fixation rates obtained through different measurement methods at the same months, locations, and depths reveals that the conventional ¹⁵N₂ bubble method yields lower rates in 69 % cases compared to the new ¹⁵N₂ dissolution method. This updated version of the database can facilitate future studies in marine ecology and biogeochemistry. The database is stored at the Figshare repository (https://doi.org/10.6084/m9.figshare.21677687; Shao et al., 2022).

1　Introduction

Dinitrogen (N₂) fixation is a process carried out by select prokaryotes (diazotrophs) capable of converting N₂ gas, which is not usable by most organisms, into bioavailable nitrogen (N). In the sunlit surface ocean, where dissolved inorganic forms of N such as nitrate (NO_3^-) and ammonium (NH_4^+) are scarce, N₂ fixation plays an important role in providing N that can contribute to primary production, particularly in oligotrophic regions (Wang et al., 2019; Gruber, 2008). Globally, N₂ fixation serves to compensate, at least partially, for fixed N removed via denitrification and anammox (Deutsch et al., 2007; Gruber, 2019).

Marine diazotrophs include three main types of cyanobacteria (Zehr, 2011): (1) nonheterocystous filamentous cyanobacteria (e.g., *Trichodesmium*); (2) heterocystous cyanobacteria like *Richelia*, which may form diatom–diazotroph associations (DDAs); and (3) unicellular cyanobacteria (UCYNs). Non-cyanobacterial diazotrophs (NCDs) have also been widely detected in the ocean (Bombar et al., 2016; Delmont et al., 2021; Moisander et al., 2017). However, the contribution of NCDs to marine N₂ fixation has not been directly quantified, despite a few studies that have reported N₂ fixation by putative NCDs at the cellular level (Harding et al., 2022; Bentzon-Tilia et al., 2015a).

Diazotroph abundance has been estimated from *nifH* gene copies using qPCR assays (Church et al., 2005b) or droplet digital PCR (ddPCR; Gradoville et al., 2017). The abundance of some cyanobacterial diazotrophs can also be obtained by counting them directly using microscopy-based techniques and in some cases flow cytometry. A recent work combined an image recognition pipeline with molecular mapping of the *nifH* gene to quantify diazotrophs in the Tara Oceans dataset

(Karlusich et al., 2021). Gene copies of *nifH* have been more frequently measured than microscopy-based cell counts and can be more useful when evaluating the abundance of different diazotrophic groups. Caution must be taken because there can be discrepancies between cell-count-based and *nifH*-based diazotrophic abundances (Luo et al., 2012), a finding largely attributed to large variations in the number of *nifH* copies per diazotroph cell, thus far observed particularly in *Trichodesmium* and heterocystous cyanobacteria (Sargent et al., 2016; White et al., 2018; Karlusich et al., 2021). However, a recent regional study spanning over 200 km of the North Pacific Subtropical Gyre has found a statistically significant linear correlation between the abundances of the *nifH* gene and cell counts in UCYN-B (i.e., *Crocosphaera*; linear slope = 1.82) and heterocystous cyanobacteria (*Richelia* and *Calothrix*; linear slope from 1.51–2.58) but not in *Trichodesmium* (Gradoville et al., 2022). A recent discussion highlighted the influence of the uncertainty in gene copy conversion to biomass and the need for further investigation of how to best take advantage of gene copy data for global diazotroph biogeography modeling purposes (Meiler et al., 2022; Zehr and Riemann, 2023); however, there is agreement that quantifying gene counts is a powerful tool for studying marine diazotroph distributions (Meiler et al., 2023; Zehr and Riemann, 2023). Meiler et al. (2023) proposed a number of topics of study for this field moving forward; Gradoville et al. (2022) concluded that "we hope that future studies report *nifH* : cell and explore the mechanisms controlling this ratio." Both gene-based and microscopy cell counts have innate biases, which should be elucidated in future studies.

Given the importance of N₂ fixation to ocean ecology and biogeochemistry, it is imperative that a database of up-to-date N₂ fixation and diazotrophic abundance measurements be maintained. Currently, global estimates of marine fixed N inputs calculated via the N₂ fixation rate mostly range from 100 to 170 Tg N yr⁻¹ (see summary in Zhang et al., 2020). This value, together with other bioavailable N sources to the ocean including riverine input and atmospheric deposition, is considerably lower than estimates of N losses from the ocean such as denitrification, anammox, and sediment burial (Zhang et al., 2020; Gruber, 2008; Zehr and Capone, 2021). While the overestimation of the N losses cannot be ruled out, one of possible reasons for this imbalance is the inaccurate estimation of global marine N₂ fixation due to limited spatiotemporal coverage of rate measurements and the different methods employed in N₂ fixation assays (White et al., 2020). Another possible reason is the limited knowledge of ecological niches of N₂-fixing organisms. Over the last decade, the realm of marine N₂ fixation has been expanded to include numerous non-paradigmatic habitats. Coastal (Mulholland et al., 2012; Bentzon-Tilia et al., 2015b; Mulholland et al., 2019; Tang et al., 2020; Turk-Kubo et al., 2021), subpolar (Sato et al., 2021; Shiozaki et al., 2018a), and even polar ocean regions (Blais et al., 2012; Sipler et al., 2017; Harding et al., 2018; Shiozaki et al., 2020) have demonstrated N₂

fixation. Notably, N₂ fixation in aphotic waters remains debated (Bonnet et al., 2013; Farnelid et al., 2013; Selden et al., 2021b; Rahav et al., 2013a; Hamersley et al., 2011; Benavides et al., 2018a; Moisander et al., 2017). Other studies have also suggested that NCDs may be significant contributors to marine N₂ fixation (Shiozaki et al., 2014b; Turk-Kubo et al., 2022; Geisler et al., 2020; Delmont et al., 2021; Karlusich et al., 2021; Bombar et al., 2016; Moisander et al., 2017) and may occupy different niches than cyanobacterial diazotrophs (Shao and Luo, 2022).

Luo et al. (2012) compiled the first global oceanic diazotrophic database including in situ measurements of N₂ fixation rates and cell-count-based and *nifH*-based diazotrophic abundance. Several years later, two studies supplemented the database with a collection of some newly reported diazotrophic data (Tang and Cassar, 2019; Tang et al., 2019), although a substantial amount of additional data remained to be included. Here, we present an updated version of the global oceanic diazotrophic database with data not yet compiled. We describe the database information, a summary of the data updates, measurement methods, and data distribution. Furthermore, we conduct a first-order estimation of the global oceanic N₂ fixation rate using the updated version of the database. In light of the aforementioned concerns of *nifH* : cell and various N₂ fixation methods (see Sect. 2.3), we also discuss the significance of employing different methodological approaches to estimate N₂ fixation rates and abundance metrics. We use the data available in the database to analyze the discrepancies between N₂ fixation rates using ¹⁵N₂ bubble and dissolution methods, and compare the observed ranges of *nifH* gene copies and diazotrophic cell abundance.

2 Data and methods

2.1 Database summary

This study updated the original global oceanic diazotrophic database of Luo et al. (2012; version 1 hereafter) with new in situ measurements of N₂ fixation rates and abundances of diazotrophic cells and *nifH* gene copies. Together there were 55 286 diazotrophic data points in the updated database (version 2 hereafter; Tables 1–3), including 13 565 data points from version 1 (Luo et al., 2012), 6736 measured in 2012–2018 and compiled by two previous studies (Tang et al., 2019; Tang and Cassar, 2019), 26 597 data points measured in 1979–2023 and compiled by this study, and 8388 NCD data mostly from Turk-Kubo et al. (2022; see below). In version 2, some errors in the datasets of Tang et al. (2019), mostly caused by unit conversions, were also corrected.

Version 2 was composed of six main sub-databases: (1) 9231 volumetric N₂ fixation rates (5853 new data points; Tables 1 and 4); (2) 2590 depth-integrated N₂ fixation rates (1805 new data points; Tables 1 and 4); (3) 9040 volumetric cell abundances (4154 new data points; Tables 2 and 5);

(4) 1784 depth-integrated cell abundances (859 new data points; Tables 2 and 5); (5) 29 655 volumetric *nifH* gene copy abundances (26 506 new data points; Tables 3 and 6); and (6) 2986 depth-integrated *nifH* gene copy abundances (2544 new data points; Tables 3 and 6). Please be aware that 2416 N$_2$ fixation rates were measured with incubation periods less than 24 h; they were listed in separate spreadsheets in the database for reasons discussed in Sect. 2.3. Additionally, we included a compiled NCD dataset (Turk-Kubo et al., 2022) in the database, which contained 7919 *nifH* gene copy abundances of primarily the most studied phylotype NCD Gamma A (Shao and Luo, 2022; Langlois et al., 2015), also referred to as 24774A11 (Moisander et al., 2012) and UMB (Bird et al., 2005), as well as other phylotypes, and updated the compilation with 469 additional *nifH* gene copy abundances of NCDs published more recently (Turk-Kubo et al., 2021; Sato et al., 2022; Moore et al., 2018; Reeder et al., 2022; Wen et al., 2022; Bonnet et al., 2023). We also collected 468 cell-specific in situ N$_2$ fixation rates and added them to version 2 (Table 7).

Depth-integrated data were either provided directly in published papers or calculated as part of this study for those vertical profiles with at least three volumetric data points in each profile. The measurements within a profile were first interpolated linearly with depth, with the shallowest datum representing the level between the sea surface and the depth of that datum. The profile was then integrated from the sea surface to the deepest recorded measurement. Most vertical profiles of N$_2$ fixation rates were measured within the euphotic zone, with a few studies extending measurements to several hundred meters or deeper. In these cases, we only integrated to the deepest data point above 200 m, taking into account the scarcity of aphotic N$_2$ fixation measurements in the global ocean and their controversial contribution to the global budget (Benavides et al., 2018a). As a result, it was possible that certain measurements below the euphotic zone but above 200 m were included in the integration. However, these measurements would typically have minimal impact on the depth-integrated N$_2$ fixation rates due to their low rates and limited vertical extent in this range.

N$_2$ fixation rates were measured for whole seawater samples, for different size fractions ($> 10\,\mu m$ and $< 10\,\mu m$), or specifically for *Trichodesmium* and heterocystous cyanobacteria. When whole-water N$_2$ fixation rates were not reported, total N$_2$ fixation rates were calculated as the sum of the N$_2$ fixation rates of available groups.

The cyanobacterial diazotrophic abundance data in version 2 were grouped into three taxonomic categories: *Trichodesmium*, UCYN, and heterocystous cyanobacteria. The UCYN abundance data were further grouped into UCYN-A, UCYN-B, and UCYN-C. Four sublineages of UCYN-A, including UCYN-A1, UCYN-A2, UCYN-A3, and UCYN-A4, have been identified (Thompson et al., 2014; Farnelid et al., 2016). UCYN-A1 and UCYN-A2 have significant distinctions in the sizes and species of their symbiotic hosts,

with the former living in relatively smaller hosts (Thompson et al., 2014; Martínez-Pérez et al., 2016; Cornejo-Castillo et al., 2016). Hence, in addition to recording the total *nifH* gene copy abundance of UCYN-A in our database, the *nifH* gene copy abundances of its sublineages were also included if reported. Heterocystous cyanobacterial abundance was grouped into *Richelia intracellularis* (het-1 and het-2, associated with *Hemiaulus* and *Rhizosolenia*, respectively) and *Richelia rhizosolenia* (het-3, previously named *Calothrix* sp., associated with *Chaetoceros*; Foster et al., 2022b).

Sampling information (latitude, longitude, depth, and time) was provided for each data point. Physical, chemical, and biological parameters, including temperature, salinity, and concentrations of nitrate, phosphate, iron, and chlorophyll *a*, were also included when available.

2.2 Quality control

The data of N$_2$ fixation rates and diazotrophic abundance in the database spanned several orders of magnitude. Extremely high rates and abundance values of both usually occurred during algal blooms, and zero values indicated that diazotrophic activity was below detection or truly absent at the sampling time and stations. The positive-value data were first logarithmically transformed and then analyzed for outliers, considering that they were approximately log-normally distributed (Figs. S1–S5). For each parameter, we used Chauvenet's criterion to identify suspicious outliers whose probability of deviation from the means is lower than $1/2n$, where n is the number of data points (Glover et al., 2011). Because N$_2$ fixation rates and diazotroph abundances in the ocean can be extremely low, this filtering only applied to data on the high side. Although these outliers (labeled in the database) could be true values, we flagged them to caution users.

2.3 Nitrogen fixation rate data

The commonly used methods for marine N$_2$ fixation rates include $^{15}N_2$ tracer methods and the acetylene reduction assay (Mohr et al., 2010; Montoya et al., 1996; Capone, 1993). However, in the last decade, the community has turned largely to the use of $^{15}N_2$ tracer methods. The acetylene reduction assay estimates gross N$_2$ fixation rates indirectly from the reduction of acetylene to ethylene. Theoretical conversion factors of 3 : 1 and 4 : 1 have been used to convert acetylene reduction rates to N$_2$ fixation rates (Postgate, 1998; Capone, 1993; Wilson et al., 2012), although a wide range of conversion factors from 0.93 to 56 have been reported (e.g., Mague et al., 1974; Graham et al., 1980; Montoya et al., 1996; Capone et al., 2005; Mulholland et al., 2006; Wilson et al., 2012). When using the $^{15}N_2$ tracer method, samples are incubated in seawater with $^{15}N_2$ gas; the $^{15}N / ^{14}N$ ratio of particulate nitrogen is measured at the beginning and the end of the incubation to calculate the N$_2$ fixation rate (Capone and Montoya, 2001). Most measurements using the $^{15}N_2$

Table 1. Summary of the number of data points for N_2 fixation rates by category. Measurements with incubation periods of 24 h or less are summarized separately.

	Original database		New data added in version 2				Sum	
			Tang et al. (2019)		This study			
Volumetric N₂ fixation rate								
	24 h	< 24 h	24 h	< 24 h	24 h	< 24 h	24 h	< 24 h
Trichodesmium		677			6		6	677
Heterocystous		185						185
< 10 µm	228	28	75		265	6	568	34
> 10 µm	54	36	9	21	51	6	114	63
Whole seawater	1743	427	1169	171	3782	292	6694	890
Total	2025	1353	1253	192	4104	304	7382	1849
Proportion in version 2	21.9 %	14.6 %	13.6 %	2.1 %	44.5 %	3.3 %		
Depth-integrated N₂ fixation rate								
	24 h	< 24 h	24 h	< 24 h	24 h	< 24 h	24 h	< 24 h
Trichodesmium	40	206	81	8		9	121	223
Heterocystous	1	65	80	12			81	77
< 10 µm	28	18	7	12	21	2	56	32
> 10 µm	3	32			21	2	24	34
Whole seawater	285	107	500	53	956	41	1741	201
Total	357	428	668	85	998	54	2023	567
Proportion in version 2	13.8 %	16.5 %	25.8 %	3.3 %	38.5 %	2.1 %		

Table 2. Summary of the number of data points for diazotrophic cell abundances. UCYNs include UCYN-A, UCYN-B, and unclassified UCYNs. Heterocystous cyanobacteria include Het-1, Het-2, and Het-3.

	Original database	New data added to version 2	Sum
Volumetric cell abundances			
Trichodesmium	3274	2812	6086
UCYN		139	139
Heterocystous cyanobacteria	1612	1203	2815
Total	4886	4154	9040
Proportion in version 2	54.1 %	45.9 %	
Depth-integrated cell abundances			
Trichodesmium	620	692	1312
UCYN		19	19
Heterocystous	305	148	453
Total	925	859	1784
Proportion in version 2	51.9 %	48.1 %	

tracer method only counted the fixed N in particulate forms and ignored the N that was fixed but then excreted by diazotrophs in the form of dissolved organic N (DON) during incubation, which could theoretically be counted by the acetylene reduction assays (Mulholland, 2007). In some studies using the $^{15}N_2$ tracer method, this missing N was counted by also measuring the ^{15}N enrichment in DON (Berthelot et al., 2017; Benavides et al., 2013a; Berthelot et al., 2015; Benavides et al., 2013b).

Compared to the $^{15}N_2$ tracer method, the acetylene reduction assay requires less incubation time. However, in addition to the uncertainty in converting ethylene production to N_2 fixation, the purity of acetylene gas, trace ethylene contamination, and the Bunsen gas solubility coefficient of produced ethylene can also affect the accuracy of estimated N_2 fixation rates (Hyman and Arp, 1987; Breitbarth et al., 2004; Kitajima et al., 2009). Acetylene used in the assay can even impact the metabolic activities of dia-

Table 3. Summary of the number of data points for *nifH* gene copy abundances. UCYNs include UCYN-A1, UCYN-A2, UCYN-B, and UCYN-C. Heterocystous cyanobacteria include Het-1, Het-2, and Het-3.

	Original database	New data added to version 2		Sum
		Tang and Cassar (2019)	This study	
Volumetric *nifH* gene copy abundances				
Trichodesmium	758	770	3165	4693
UCYN	1792	2640	6903	11 309
Heterocystous cyanobacteria	599	505	4135	5239
NCDs			8388	8388
Total	3149	3915	22 591	29 655
Proportion in version 2	10.6 %	13.2 %	76.2 %	
Depth-integrated *nifH* gene copy abundances				
Trichodesmium	105	123	408	636
UCYN	263	418	871	1552
Heterocystous	74	82	642	798
Total	442	623	1921	2986
Proportion in version 2	14.8 %	20.9 %	64.3 %	

zotrophs (Giller, 1987; Hardy et al., 1973; Flett et al., 1976; Staal et al., 2001). Moreover, the acetylene reduction assay needs to preconcentrate cells for signal detection when diazotrophic biomass is low, which may lead to underestimated N₂ fixation rates by perturbing cells during concentration and filtration (e.g., Capone et al., 2005; Barthel et al., 1989; Staal et al., 2007). In recent years, the acetylene reduction assay has undergone significant advancement. The sensitivity of ethylene detection has been improved by utilizing a reduced gas analyzer (Wilson et al., 2012) and by using highly purified acetylene gas to minimize the ethylene background (Kitajima et al., 2009). However, preparing high-purity acetylene with a low level of ethylene contamination remains a challenge. More recently, a new method named Flow-through incubation Acetylene Reduction Assays by Cavity ring-down laser Absorption Spectroscopy (FARACAS) has been introduced for high-frequency measurements of aquatic N₂ fixation (Cassar et al., 2018). This method involves continuous flow-through incubations and spectral monitoring of acetylene reduction to ethylene. By employing short-duration flow-through incubations without cell preconcentration, potential artifacts are minimized. This approach also allows for near-real-time estimates, enabling adaptive sampling strategies.

The original $^{15}N_2$ tracer method involves the addition of a known volume of $^{15}N_2$-labeled bubbles to the incubation bottle (named *original $^{15}N_2$ bubble method* hereafter). However, this method was found to underestimate rates because N₂ gas solubility is low and tracer additions take a long time to equilibrate (Mohr et al., 2010; Großkopf et al., 2012; Jayakumar et al., 2017). To address this issue, the $^{15}N_2$ *dissolution method* has been employed, which involves pre-preparing $^{15}N_2$-enriched seawater to maintain constant $^{15}N_2$ atom %

enrichment throughout the incubation (Mohr et al., 2010), similar to the method described in Glibert and Bronk (1994). However, the $^{15}N_2$ dissolution method does not always yield higher N₂ fixation rates than the original $^{15}N_2$ bubble method (Table S4 in Großkopf et al., 2012; Saulia et al., 2020); it is still not conclusive what controls the magnitude of the underestimation (if it exists) in the original $^{15}N_2$ bubble method. Compared to the original $^{15}N_2$ bubble method, the $^{15}N_2$ dissolution method is more susceptible to the introduction of contaminants (e.g., metals) during the preparation of the $^{15}N_2$ inoculum due to its more complex process, which can alter the diazotrophic activities and abundance, thereby impacting the accuracy of N₂ fixation measurements (Dabundo et al., 2014; Klawonn et al., 2015). For example, Needoba et al. (2007) reported that a low but detectable amount of Fe^{3+} contamination can be measured when protecting the needle of the gas-tight syringe with commercially available tubing. Additionally, pH and other chemical properties of the inoculum may be altered during its preparation, further affecting the measurements of N₂ fixation. Despite these limitations, the $^{15}N_2$ dissolution method remains the predominant assay for measuring N₂ fixation rate due to its ability to satisfy the fundamental assumption of constant $^{15}N_2$ atom % enrichment over the incubation period.

More recently, a modified $^{15}N_2$ bubble method, known as the $^{15}N_2$ *bubble release method*, has been proposed as an alternative to the $^{15}N_2$ dissolution method (Klawonn et al., 2015; Chang et al., 2019; Selden et al., 2019). This method involves adding $^{15}N_2$ gas to the incubation bottles and mixing for a brief period ($\sim$ 15 min) to facilitate $^{15}N_2$ equilibration and then removing the gas bubble. Compared to the original $^{15}N_2$ bubble method, the $^{15}N_2$ bubble release method ensures uniform $^{15}N_2$ atom % enrichment throughout the in-

Table 4. Summary of new data points of N$_2$ fixation rates added to version 2 of the database.

Reference	Region	*Trichodesmium*	Heterocystous	< 10 µm diazotrophs	> 10 µm diazotrophs	Whole seawater	Depth-integrated data
Part 1. Incubation periods of 24 h							
Ahmed et al. (2017)	E Arabian Sea					19	5[a]
Benavides et al. (2016b)	Mediterranean Sea					10	
Benavides et al. (2018a)	Tropical SW Pacific					59	
Benavides et al. (2022b)	Tropical SW Pacific					38	
Benavides et al. (2017)	SW Pacific					2	
Benavides et al. (2021)	S Pacific					41	
Benavides et al. (2022a)	S Pacific	6				6	2
Bentzon-Tilia et al. (2015b)	Baltic Sea					23	23[a]
Berthelot et al. (2017)	Tropical W Pacific					48	12[a]
Biegala and Raimbault (2008)	SW Pacific			12	12	12	9
Blais et al. (2012)	Arctic Ocean					18	12
Bombar et al. (2015)	Subtropical N Pacific					20	2
Bonnet et al. (2013)	Tropical SE Pacific						8[a]
Bonnet et al. (2018)	Tropical SW Pacific					102	14
Bonnet et al. (2015)	SW Pacific			126		128	30[a]
Bonnet et al. (2023)	Subtropical S Pacific					84	14
Böttjer et al. (2017)	Subtropical N Pacific					243	108[a]
Cerdan-Garcia et al. (2021)	Subtropical N Atlantic					15	
Chang et al. (2019)	Tropical SE Pacific					37	
Chen et al. (2019)	W Pacific Ocean					95	16
Dekaezemacker et al. (2013)	Tropical SE Pacific					43	10
Dugenne et al. (2023)	Subtropical N Pacific					30	5
Fernandez et al. (2015)	Central Chile upwelling system					55	14[a]
Fernández-Castro et al. (2015)	Atlantic, Pacific, and Indian oceans					177	43[a]
Fonseca-Batista et al. (2017)	E Atlantic					56	14
Fonseca-Batista et al. (2019)	Temperate NE Atlantic					46	10[a]
Foster et al. (2009)	Red Sea					26	
Foster et al. (unpublished data)	E tropical S Pacific					23	5
Garcia et al. (2007)	SW Pacific						1[a]
Gradoville et al. (2020)	N Pacific					20	
Gradoville et al. (2017)	S Pacific; N Pacific					30	5
Großkopf et al. (2012)	Atlantic Ocean					39	17
Hallstrøm et al. (2022)	NE Atlantic					59	11[a]
Harding et al. (2018)	Arctic Ocean					38	
Harding et al. (2022)	Subtropical N Pacific					7	
Hörstmann et al. (2021)	S Indian Ocean; Southern Ocean					13	
Ibello et al. (2010)	Mediterranean Sea					21	14[a]
Jayakumar et al. (2017)	Tropical NE Pacific					32	7
Jiang et al. (2023)	East China Sea and Southern Yellow Sea					97	29[a]
Kittu et al. (2023)	Tropical SE Pacific					103	21
Knapp et al. (2016)	Tropical SE Pacific						6[a]
Konno et al. (2010)	NW Pacific						16[a]
Krupke et al. (2015)	Subtropical NE Atlantic					1	
Kumari et al. (2022)	Bay of Bengal					97	18[a]
Landou et al. (2023)	Red Sea					72	22[a]
Li et al. (2020)	N South China Sea; East China Sea					68	15[a]
Liu et al. (2020)	South China Sea					25	5[a]
Loescher et al. (2014)	Tropical SE Pacific					30	5[a]
Loick-Wilde et al. (2015)	Amazon River						54[a]
Loick-Wilde et al. (2019)	Tropical W Pacific					8	
Lory et al. (2022)	Tropical SE Pacific					5	
Löscher et al. (2016)	Tropical SW Pacific					225	31 + 4[a]
Löscher et al. (2020)	Bay of Bengal					18	
Lu et al. (2018)	Equatorial W Pacific					3	3[a]
Martínez-Pérez et al. (2016)	Tropical N Atlantic					84	14
Messer et al. (2016)	S Pacific					27	
Messer et al. (2021)	S Australian gulf system			10		10	
Mills et al. (2020)	California Current System					4	
Moreira-Coello et al. (2017)	Coastal NW Iberian upwelling			30			10[a]
Mulholland et al. (2019)	NW Atlantic					402	242[a]
Needoba et al. (2007)	Temperate N Pacific					2	
Palter et al. (2020)	Gulf Stream					7	
Raes et al. (2014)	E Indian					31	
Raes et al. (2020)	S Pacific					118	
Rahav et al. (2013a, 2015)	Red Sea and E Mediterranean Sea					62	10
Rahav et al. (2013b)	Mediterranean Sea					8	
Rahav et al. (2016)	Mediterranean Sea						3[a]
Reeder et al. (2022)	S Baltic Sea					15	5

Table 4. Continued.

Reference	Region	*Trichodesmium*	Heterocystous	< 10 µm diazotrophs	> 10 µm diazotrophs	Whole seawater	Depth-integrated data
Riou et al. (2016)	N Atlantic					24	6
Sarma et al. (2020)	Bay of Bengal					2	
Sato et al. (2021)	Subarctic Sea of Japan; Sea of Okhotsk					31	3
Sato et al. (2022)	E Indian					73	18[a]
Saulia et al. (2020)	Tropical SW Pacific					71	71[a]
Selden et al. (2019)	Tropical NE Pacific					8	16[a]
Selden et al. (2021a)	NW Atlantic					93	26[a]
Selden et al. (2021b)	Tropical SE Pacific					125	19
Shiozaki et al. (2013)	W Pacific					50	10
Shiozaki et al. (2014c)	SW Pacific			40		42	
Shiozaki et al. (2014b)	Indian Ocean			26		26	6[a]
Shiozaki et al. (2015a)	NW Pacific					73	11
Shiozaki et al. (2015b)	N Pacific					112	22[a]
Shiozaki et al. (2017)	N Pacific					74	15[a]
Shiozaki et al. (2018b)	W Arctic					84	21[a]
Shiozaki et al. (2018a)	S Pacific					65	15[a]
Shiozaki et al. (2020)	Antarctic Coast					53	15
Singh et al. (2017)	Tropical NE Atlantic					52	13
Sipler et al. (2017)	Arctic Ocean					8	
Sohm et al. (2011)	S Atlantic					12	3[a]
Subramaniam et al. (2008)	Tropical N Atlantic						242[a]
Subramaniam et al. (2013)	Atlantic Ocean					96	24[a]
Tang et al. (2020)	N Atlantic					15	
Turk-Kubo et al. (2012)	Tropical N Atlantic			27			7
Turk-Kubo et al. (2021)	Southern California Current System			21		64	14
Wasmund et al. (2015)	S Atlantic						66[a]
Watkins-Brandt et al. (2011)	N Pacific						1[a]
Wen et al. (2022)	Tropical NW Pacific					143	22[a]
White et al. (2018)	Subtropical N Pacific					43	13[a]
Wilson et al. (2012)	N Pacific					9	4[a]
Wilson et al. (2017)	Subtropical N Pacific					33	
Wu et al. (2021)	Eastern Indian Ocean			48	48	48	7
Yogev et al. (2011)[b]	E Mediterranean Sea					16	32[a]
Zhang et al. (2015)	South China Sea					82	11
Zhang et al. (2019)	Tropical NW Pacific					87	9[a]
Part 2. Incubation period less than 24 h							
Agawin et al. (2013)	Subtropical Atlantic				21	17	
Benavides et al. (2013b)	Subtropical N Atlantic					38	
Benavides et al. (2014)	Coastal Namibian upwelling system					14	3
Bhavya et al. (2016)	Arabian Sea					4	
Biegala and Raimbault (2008)	SW Pacific			6	6	6	6
Bombar et al. (2011)	South China Sea					15	
Fernandez et al. (2015)	Central Chile upwelling system					29	
Foster et al. (2013)	Subtropical N Pacific					3	
Foster et al. (2022a)	Tropical NW Atlantic					45	9
Foster et al. (unpublished data)	N Atlantic					24	5
Gandhi et al. (2011)	E Arabian Sea					28	7[a]
Halm et al. (2012)	S Pacific					43	10[a]
Kromkamp et al. (1997)	Indian Ocean						9[a]
Krupke et al. (2013)	Subtropical N Atlantic					6	
Krupke et al. (2014)	N Atlantic					42	44[a]
Kumar et al. (2017)	E Arabian Sea					12	3
Chen et al. (2014)	South China Sea						24[a]
Sahoo et al. (2021)	Bay of Bengal						6[a]
Saxena et al. (2020)	Bay of Bengal					32	8[a]
Singh et al. (2019)	E Arabian Sea					20	5[a]
Wang et al. (2021)	NW Atlantic					85	
Total		6	0	346	87	5414	1805

[a] Data are reported by data providers as depth-integrated N₂ fixation rates (unlabeled data computed by integrating profiles of volumetric N₂ fixation rate data). [b] N₂ fixation rate incubation time for 24–30 h.

Table 5. Summary of new data points of cell-count-based abundances added to version 2 of the database. The data were measured using the microscopy-based method (method A), TSA/catalyzed reporter deposition fluorescence in situ hybridization (CARD-FISH; method B), flow cytometer (method C), or image recognition (method D). UCYNs include UCYN-A, UCYN-B, and unclassified UCYNs. Heterocystous cyanobacteria include Het-1, Het-2, and Het-3.

Reference	Region	Method	*Trichodesmium*	UCYN	Heterocystous cyanobacteria	Depth-integrated data
Biegala and Raimbault (2008)	SW Pacific	B		15		
Bif and Yunes (2017)	S Atlantic	A	16			
Campbell et al. (2005)	SW Pacific	A	462		259	33*
Detoni et al. (2016)	S Atlantic	A	14			
Dugenne et al. (2023), Gradoville et al. (2022)	N Pacific Subtropical Gyre	C	4	4	7	
Dupouy et al. (2011)	SW Pacific	A	18			
Estrada et al. (2016)	Global	A	407		407	
Fernández et al. (2010)	Global	A				40*
Foster et al. (2022a)	W tropical N Atlantic	A			37	9
Foster et al. (unpublished data)	N Atlantic	A			54	
Hegde et al. (2008)	Bay of Bengal	A	135			
Holl et al. (2007)	N Atlantic	A				10*
Jiang et al. (2017)	E China Sea	A	1174			252*
Jiang et al. (2023)	E China Sea	A	39		39	78*
Krupke et al. (2013)	N Atlantic	B		9		
Le Moal and Biegala (2009)	Mediterranean Sea	B		17		
Le Moal et al. (2011)	Mediterranean Sea	B		18		
Lory et al. (2022)	S Pacific	A	3			
Lu et al. (2018)	W Eq. Pacific	A	2			
Martínez-Pérez et al. (2016)	Tropical N Atlantic	A		56		14
Masotti et al. (2007)	SW Pacific	A	20			5
Mompeán et al. (2013)	N Atlantic	A				43*
Mompeán et al. (2016)	Global	A				141*
Karlusich et al. (2021)	Global	D	46		81	
Riou et al. (2016)	N Atlantic	B		20		5
Sahu et al. (2017)	Bay of Bengal	A	14			
Shiozaki et al. (2013)	W Pacific	A	10		12	
Shiozaki et al. (2015a)	NW Pacific	A	60			10
Subramaniam et al. (2008)	N Atlantic	A				162*
Tenório et al. (2018)	SW Pacific	A	81			19*
White et al. (2018)	N Pacific	A	83		83	38
Wu et al. (2021)	Bay of Bengal	A	224		224	
Total			2812	139	1203	859

* Data are reported by data providers as depth-integrated cell abundance (unlabeled depth-integrated abundances computed from volumetric data).

cubation. Moreover, it causes less interference with the incubation matrix than the ^{15}N$_2$ dissolution method. However, the mixing of incubation bottles required to stimulate gas dissolution has been suggested to negatively affect diazotrophs, although no robust studies have yet been performed to assess this critique (Wannicke et al., 2018; White et al., 2020). Moreover, the ^{15}N$_2$ bubble release method requires a handling step, and additional costs for preparing tracers may be another challenge for researchers (White et al., 2020). Ultimately, White et al. (2020) "advise employing either the dissolution or bubble release method, whichever is best suited to the specific research objectives and logistical constraints" with additional recommendations on the need for determination of detection limits for all rate measurements.

We compared volumetric N$_2$ fixation rates in the upper 50 m and depth-integrated N$_2$ fixation rates in the database measured using acetylene reduction assays, the original ^{15}N$_2$
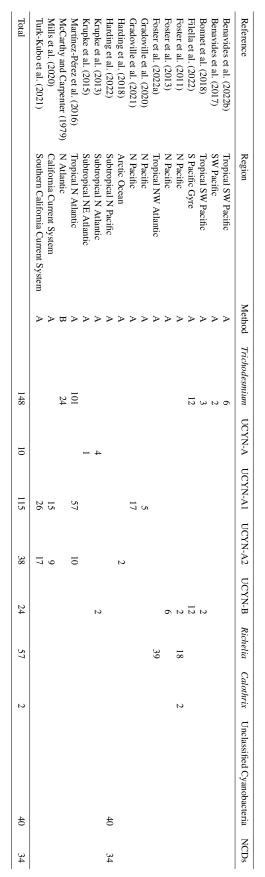
bubble method, and the ^{15}N$_2$ dissolution method and found that they span a similar range (Fig. 1). Meanwhile, in the analysis for volumetric N$_2$ fixation rates in the upper 50 m, the peak of the log-normal distributions of the measurements using the ^{15}N$_2$ dissolution method was approximately double that of the original ^{15}N$_2$ bubble method (Fig. 1a). The measurements using the ^{15}N$_2$ bubble release method were limited to several study sites and their distribution was thus not presented in this study. A further analysis comparing the original ^{15}N$_2$ bubble method and the ^{15}N$_2$ dissolution method will be presented later (see Sect. 4.1).

The majority of N$_2$ fixation rates (9405) were measured with incubation periods of 24 h and were reported as daily rates. In contrast, 2416 samples were incubated for less than 24 h and hourly N$_2$ fixation rates were reported. Diel cycles of N$_2$ fixation vary among samples and/or diazotrophic groups, and substantial errors may be introduced when ex-

Table 6. Summary of new data points of *nifH* gene copy abundances added to version 2 of the database. UCYNs include UCYN-A1, UCYN-A2, UCYN-B, and UCYN-C. Heterocystous cyanobacteria include Het-1, Het-2, and Het-3.

Reference	Region	*Trichodesmium*	UCYN	Heterocystous cyanobacteria	Depth-integrated data
Benavides et al. (2016b)	N Atlantic	13	30	15	
Bentzon-Tilia et al. (2015b)	Baltic Sea		20		
Berthelot et al. (2017)	Tropical W Pacific	64	256	64	96
Bombar et al. (2011)	South China Sea	18	36	18	
Bombar et al. (2015)	N Pacific				32
Bonnet et al. (2015)	SW Pacific	87	261	87	84
Bonnet et al. (2023)	SW Pacific	66	132		44
Cabello et al. (2020)	Monterey Bay		200		
Confesor et al. (2022)[b]	W Florida Shelf	67			
Cerdan-Garcia et al. (2021)	N Atlantic	7	7		
Chen et al. (2019)	W Pacific	103	381	177	123
Cheung et al. (2020)	N Pacific	519	519		
Cheung et al. (2022)	W Bering Sea		58	29	
Church and Zehr (2020)	N Pacific	968	1936	1936	605
Church et al. (2008)	N Pacific				60
Detoni et al. (2022)	SW Atlantic	70	140	70	72
Dugenne et al. (2023), Gradoville et al. (2022)	N Pacific Subtropic Gyre	72	216	216	112
Foster et al. (unpublished data)	South China Sea	99	224	350	158
Gradoville et al. (2020)	N Pacific	43	85	28	
Hallstrøm et al. (2022)	NE Atlantic				42[a]
Halm et al. (2012)	S Pacific Gyre	8	16		
Hamersley et al. (2011)	S California Bight	6	12	6	
Harding et al. (2018)	Arctic Ocean		39		
Hashimoto et al. (2016)	Seto Inland Sea		176		
Henke et al. (2018)	Tropical SW Pacific		142		
Krupke et al. (2013)	N Atlantic		24		3
Liu et al. (2020)	South China Sea	49	98		33
Lory et al. (2022)	Tropical SW Pacific	3	3		
Lu et al. (2018)	Tropical W Pacific	3	6	3	
Martínez-Pérez et al. (2016)	Tropical N Atlantic	84	252	84	70
Messer et al. (2021)	S Australian Gulf		20		
Mills et al. (2020)	Coast of S California	4	12	4	
Moisander et al. (2014)	S Pacific	174	348	174	92
Moore et al. (2018)	Tropical Atlantic	104	312	208	
Moreira-Coello et al. (2017)	Coastal NW Iberian upwelling		20		20[a]
Palter et al. (2020)	Gulf Stream	24	24		
Ratten et al. (2015)	N Atlantic	9	27	9	10
Reeder et al. (2022)	Baltic Sea		15	15	
Sato et al. (2021)	Subarctic Sea		31		3
Sato et al. (2022)	Eastern Indian Ocean	73	73		36
Saulia et al. (2020)	SW Pacific	71	213	143	
Scavotto et al. (2015)	N Atlantic		2		
Selden et al. (2021a)	Atlantic Bight	23	69	23	
Selden et al. (2022)	Arctic Ocean		40		
Shiozaki et al. (2014b)	Arabian Sea	26	52		18
Shiozaki et al. (2014a)	S China Sea	171	342		72[a]
Shiozaki et al. (2015a)	Temperate N Pacific	73	146		33
Shiozaki et al. (2017)	N Pacific	74	222	74	90
Shiozaki et al. (2018c)	Kuroshio	46	138	46	
Shiozaki et al. (2018b)	W Arctic		84		21
Shiozaki et al. (2018a)	S Pacific	94	285	95	95
Shiozaki et al. (2020)	Antarctic sea ice		53		
Sohm et al. (2011)	S Atlantic Gyre		58		
Stenegren et al. (2017)	Tropical NW Atlantic			235	61
Stenegren et al. (2018)	Tropical SW Pacific	108	402	120	108
Tang et al. (2020)	N Atlantic	42	42		
Turk-Kubo et al. (2014)	Tropical SE Pacific	60	159	57	53
Turk-Kubo et al. (2021)	Coast of S California	190	588	202	135
Wen et al. (2017)	W Pacific	22	44	22	
Wen et al. (2022)	W Pacific	130	390	130	110[a]
White et al. (2018)	N Pacific				34
Wu et al. (2019)	Bay of Bengal	68	63		19
Total		3935	9543	4640	2544

[a] Data are reported by data providers as depth-integrated *nifH* gene copy abundances (unlabeled depth-integrated abundances computed from volumetric data). [b] *rnpB* gene copies were determined.
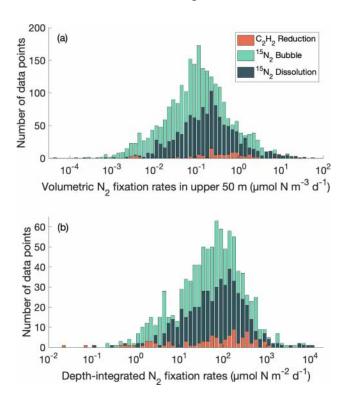
Figure 1. Distribution of N$_2$ fixation rates measured using acetylene (C$_2$H$_2$) reduction assays, the original ^{15}N$_2$ bubble method, and the ^{15}N$_2$ dissolution method. **(a)** Volumetric data in the upper 50 m; **(b)** depth-integrated data. Only rates measured with incubation periods of 24 h are shown. Please note that the bars in the plots do not represent cumulative data.

Table 7. Summary of data points of cell-specific N$_2$ fixation rates added to version 2 of the database. The rates were measured either by using the combination of CARD-FISH and nanoscale secondary ion mass spectrometry (nanoSIMS; method A) or via the measurements of bulk N$_2$ fixation rates incubated with a known number of diazotrophic cells (method B; see Sect. 2.3). Note that all the data were reported as N$_2$ fixation rates per cell, except for Filella et al. (2022) in which biomass-normalized rates in units of d^{-1} were reported.

Reference	Region	Method	*Trichodesmium*	UCYN-A	UCYN-A1	UCYN-A2	UCYN-B	*Richelia*	*Calothrix*	Unclassified Cyanobacteria	NCDs
Benavides et al. (2022b)	Tropical SW Pacific	A	6								
Benavides et al. (2017)	SW Pacific	A	2								
Bonnet et al. (2018)	Tropical SW Pacific	A	3				2				
Filella et al. (2022)	S Pacific Gyre	A	12				12		2		
Foster et al. (2011)	N Pacific	A					2				
Foster et al. (2013)	N Pacific	A					6				
Foster et al. (2022a)	Tropical NW Atlantic	A		5							
Gradoville et al. (2020)	N Pacific	A						39			
Gradoville et al. (2021)	N Pacific	A						18			
Harding et al. (2018)	Arctic Ocean	A					2				
Harding et al. (2022)	Subtropical N Pacific	A				2					
Krupke et al. (2013)	Subtropical NE Atlantic	A		4							
Krupke et al. (2015)	Tropical N Atlantic	A	101	1	57	10					
Martínez-Pérez et al. (2016)	N Atlantic	B	24		15	9					
McCarthy and Carpenter (1979)	California Current System	A									
Mills et al. (2020)	California Current System	A			26	17					
Turk-Kubo et al. (2021)	Southern California Current System	A			17					40	34
Total			148	10	115	38	24	57	2	40	34

trapolating N$_2$ fixation rates incubated for less than 24 h to daily rates (White et al., 2020). Therefore, the N$_2$ fixation rates measured with incubation periods of less than 24 h were collected into separated data sheets in our database and were not used in further analysis within this study. Please note that the incubation periods of whole diurnal cycles (e.g., 24, 48, or 72 h) were used in Konno et al. (2010). The incubation of samples in Yogev et al. (2011) lasted from 24 to 30 h. The reported daily N$_2$ fixation rates by these two studies were also included in the 24 h data sheets and were used in our estimation of the global marine N$_2$ fixation rate (see below).

Cell-specific N$_2$ fixation rates of diazotrophs (or symbioses) were mostly measured using catalyzed reporter deposition fluorescence in situ hybridization (CARD-FISH) and nanoscale secondary ion mass spectrometry (nanoSIMS), in combination with ^{15}N$_2$ addition experiments (Mills et al., 2020; Berthelot et al., 2019). Using specific oligonucleotide probes, CARD-FISH enables the visualization and location of the regions of interest in diazotrophs at a single-cell level using a epifluorescence microscope. This is subsequently prepared for the secondary electron image in nanoSIMS analysis. Importantly, the handling, fixation, and processing of the samples with CARD-FISH has been demonstrated to significantly impact the enrichment measured by nanoSIMS
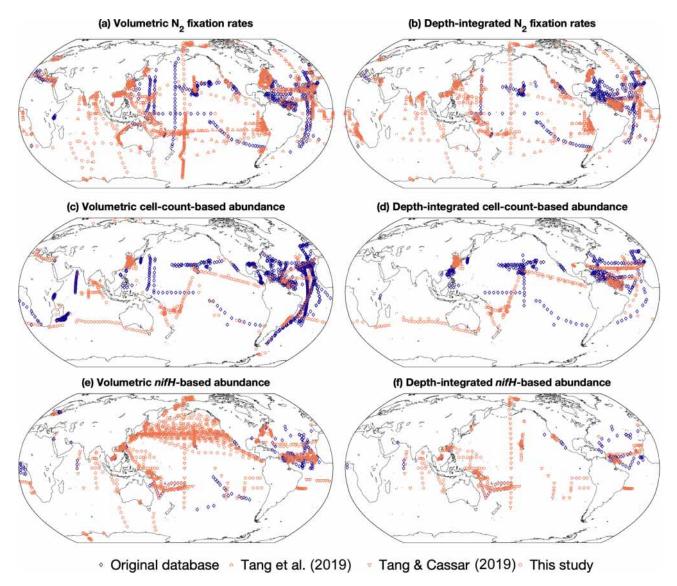
Figure 2. Spatial distribution of the number of volumetric and depth-integrated data points in version 2 of the diazotrophic database, binned in 1° latitude × 1° longitude grids. **(a, b)** N₂ fixation rates, **(c, d)** cell abundance, and **(e, f)** *nifH* gene copy abundance. The data sources include the original version of this database (Luo et al., 2012; blue diamonds), two compiled datasets (Tang et al., 2019; Tang and Cassar, 2019; orange triangles), and this study (orange circles).

(see Musat et al., 2014; Woebken et al., 2015; Meyer et al., 2021). The nanoSIMS technique detects the enrichment of ^{15}N atoms in the targeted regions, allowing for the calculation of the cell-specific rate. Additionally, in one study, hand-picked *Trichodesmium* colonies or trichomes were incubated and the measured total N₂ fixation rates were normalized to number of cells (McCarthy and Carpenter, 1979).

2.4 Estimation of the global marine N₂ fixation rate

Using these data, we performed a first-order estimation of the global marine N₂ fixation rate. In a previous study (Luo et al., 2012), version 1 was utilized to estimate the global marine N₂ fixation rate, which included all the depth-integrated N₂

fixation rates. However, in this study, we employed more rigorous criteria to estimate the global rate using both version 1 and version 2, taking into account the reliability of different N₂ fixation rate data discussed in the preceding section. Specifically, we exclusively used depth-integrated N₂ fixation rates that met the following criteria: (1) measurements were taken from whole seawater samples, (2) incubation periods of 24 h were used, and (3) the three ^{15}N₂-based methods were employed, although we acknowledged that the rates obtained using the original ^{15}N₂ bubble method might be underestimated. N₂ fixation rates obtained through the acetylene reduction method were excluded from this estimate due to the significant uncertainties described above.

Figure 3. Spatial distribution of the number of volumetric and depth-integrated data points binned in 1° latitude × 1° longitude grids for **(a, b)** N$_2$ fixation rates, **(c, d)** cell abundance, and **(e, f)** *nifH* gene copy abundance. The size of the circles represents the number of data points in each bin. The blue diamonds mark the location of outliers identified using Chauvenet's criterion.

Applying these criteria, we selected 309 and 1642 depth-integrated N$_2$ fixation rates from version 1 and version 2, respectively. The greater number of data in version 2 potentially provided more constraints on estimating global marine N$_2$ fixation. We applied Chauvenet's criterion to identify outliers, using the log-transformed values of the selected data (see Sect. 2.2). As a result, two high-value outliers were removed in version 1 (one in the North Pacific and one in the South Pacific) while no outliers were detected in version 2. This difference can be attributed to the larger number of data samples in version 2, which allowed for a more relaxed threshold in identifying outliers.

The estimation of the global marine N$_2$ fixation rate involved four steps. First, we calculated the arithmetic or geometric means of the depth-integrated N$_2$ fixation rates within each 3° latitude × 3° longitude bin. Second, these mean values were further averaged using either arithmetic or geometric methods to determine the mean N$_2$ fixation rates for different ocean basins, which included the North Atlantic, South Atlantic, North Pacific, South Pacific, Indian, Arctic, and Southern oceans, as well as the Mediterranean Sea. Third, we multiplied the arithmetic or geometric mean of each basin by its respective area to estimate the total N$_2$ fixation rate for that specific basin, except when there was insufficient spatial coverage available. Finally, we obtained the global marine

Figure 4. Latitudinal distribution of volumetric and depth-integrated **(a, b)** N$_2$ fixation rates, **(c, d)** cell abundance, and **(e, f)** *nifH* gene copy abundance, including the data from version 1 of the database (blue) and the new data added to version 2 of the database (orange).

N$_2$ fixation rate by summing up the individual rates calculated for each basin, with the errors associated with the basin rates propagated properly (Glover et al., 2011).

In the first two steps, the geometric means were derived from positive N$_2$ fixation rates (NF$_+$): if μ and SE represented the mean and standard error of $\ln(\mathrm{NF}_+)$, respectively, the geometric mean was e^μ. The confidence interval for the geometric mean, based on the standard error, ranged between e^μ/e^{SE} and $e^\mu \cdot e^{\mathrm{SE}}$ (Thomas, 1979). To address the issue of not including zero-value N$_2$ fixation rates, we adjusted the geometric means by multiplying them with the percentage of zero-value data within each 3° latitude × 3° longitude bin (in the first step) or within each basin (in the second step).

2.5 Diazotrophic abundance data

Diazotroph cell abundances were determined by using standard light microscopy, and in some cases by using epifluorescence microscopy. A recent study used machine learning techniques to detect and enumerate diazotrophs in a large dataset of microscopic images (Karlusich et al., 2021). In the original database, only the cell abundances of *Trichodesmium* and heterocystous cyanobacteria were recorded.

Version 2 also included datasets of enumerated abundance of all UCYN groups detecting them by tyramide signal amplification–FISH (TSA-FISH) using a specific DNA probe UCYN-238 (Biegala and Raimbault, 2008; Le Moal and Biegala, 2009; Le Moal et al., 2011; Riou et al., 2016). This method is also called CARD-FISH and was used specifically to enumerate UCYN-A (Martínez-Pérez et al., 2016; Biegala and Raimbault, 2008; Le Moal et al., 2011; Table 5).

Cell abundance of *Trichodesmium* was recorded as the number of trichomes per volume of water in our database, although it was also reported in some studies as the number of cells or colonies per volume of water. In the latter cases, the data were converted to trichomes per volume of water by using a commonly used factor of 200 (132–241) trichomes colony^{-1} (Letelier and Karl, 1996), similar to the conversion used in the original database (Luo et al., 2012).

The abundance of heterocystous cyanobacterial cells was also recorded in this database. Based on the number of DDAs was reported in several studies, we assumed that two (reported range: 1–2) and five (reported range: 1–5) *Richelia* spp. filaments were associated with each *Hemiaulus* and *Rhizosolenia* cell, respectively (Villareal et al., 2011; Caputo et al., 2019), and that five (reported range: 3–10) *Richelia rhi-*
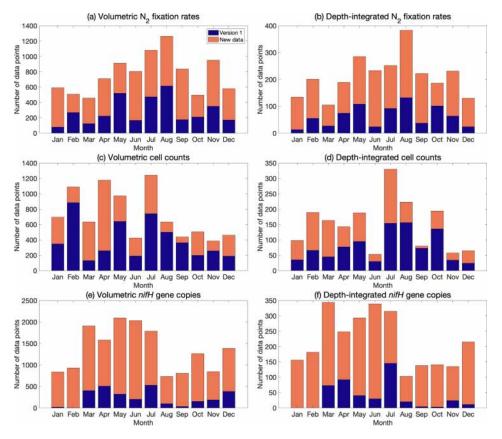
Figure 5. Monthly distribution of volumetric and depth-integrated **(a, b)** N$_2$ fixation rates, **(c, d)** cell abundance, and **(e, f)** *nifH* gene copy abundance, including the data from version 1 of the database (blue) and the new data added to version 2 of the database (orange).

zosolenia filaments were associated with each *Chaetoceros* cell (Tuo et al., 2021; Caputo et al., 2019). *Richelia* have terminal heterocysts, and the number of vegetative cells varies depending on the host diatom. In *Hemiaulus* and *Chaetoceros* spp. diatoms, *Richelia* filaments are shorter (e.g., 3–4 vegetative cells) compared to in *Rhizosolenia*, where *Richelia* filaments are longer (e.g., 5–6 vegetative cells; Foster et al., 2022b).

In measurements of *nifH* gene copy abundances, different qPCR or ddPCR assays were designed to target specific diazotrophic groups (Church et al., 2005a; Foster et al., 2007; Gradoville et al., 2017; Benavides et al., 2016b), mainly including *Trichodesmium*, UCYN subgroups (A1, A2, B, and C) and heterocystous groups (het-1, het-2, and het-3; Table 6).

All the uncertainties reported in this paper reflect one standard error of the means unless specified.

3 Results

3.1 Data distribution

Version 2 of the database significantly expanded N$_2$ fixation rate measurements, filling spatial gaps, particularly in the In-

dian Ocean and the Southern Hemisphere (Table 1; Figs. 2a and b, 3a and b). The number of depth-integrated N$_2$ fixation rate measurements was tripled (Table 1; Figs. 2b and 3b). The largest fraction of new data derived from inclusion of *nifH* gene abundances, in particular data contributions from the Pacific and Atlantic oceans (Table 3; Figs. 2e and f, 3e and f). Compared to other parameters, the new database contained only a modest increase in new cell abundances, mostly from subtropical oceans (Table 2; Figs. 2c and d, 3c and d). Overall, there remained more limited data on N$_2$ fixation and diazotrophic abundance in the Arctic and Southern oceans, with a number of rate measurements reporting values below detection limits.

Version 2 added data at all latitudinal ranges (Fig. 4). In particular, version 2 extended the range of data from tropical and subtropical areas to include polar regions in the Arctic Ocean (Harding et al., 2018) and Antarctic coast (Shiozaki et al., 2020).

The data in version 2 reduce the difference in the number of data points across months, especially for *nifH* gene copies, in which substantially more samples were collected in January and February (Fig. 5). When considering seasons in both the Northern Hemisphere and the South Atlantic and Pacific, the data were distributed more evenly (Fig. 6).
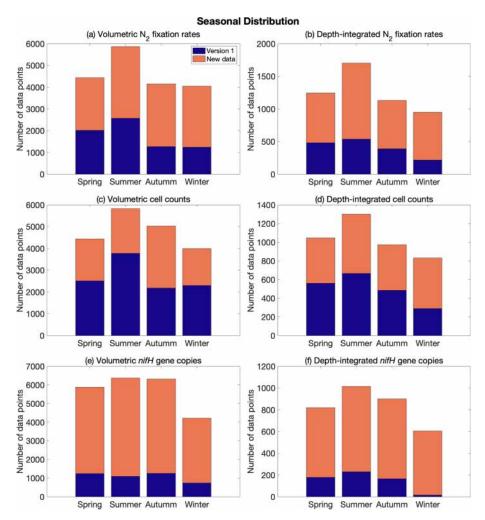
Figure 6. Seasonal distribution of volumetric and depth-integrated **(a, b)** N$_2$ fixation rates, **(c, d)** cell abundance, and **(e, f)** *nifH* gene copy abundance, including the data from version 1 of the database (blue) and the new data added to version 2 of the database (orange). Spring: March–May in the Northern Hemisphere and September–November in the Southern Hemisphere; summer: June–August in the Northern Hemisphere and December–February in the Southern Hemisphere; autumn: September–November in the Northern Hemisphere and March–May in the Southern Hemisphere; and winter: December–February in the Northern Hemisphere and June–August in the Southern Hemisphere.

Although most of the new data were measured in near-surface waters, numerous *nifH* gene copy abundance data were also sampled in deeper layers in the euphotic zone (Fig. 7). Additionally, active N$_2$ fixation and the existence of diazotrophs were found below the euphotic zone (e.g., depth > 200 m; Benavides et al., 2016a, 2018b; Selden et al., 2019; Hamersley et al., 2011; Bonnet et al., 2013; Loescher et al., 2014; Benavides et al., 2015; Fig. 7).

3.2 N$_2$ fixation rates

The volumetric N$_2$ fixation rates in five vertical layers and the depth-integrated N$_2$ fixation rates were binned in 3° latitude × 3° longitude bins, and the arithmetic means in each bin are displayed (Fig. 8). The depth-integrated N$_2$ fixation rates ranged over orders of magnitude, from 10^{-4}–

$10^3\,\mu\mathrm{mol\,N\,m^{-2}\,d^{-1}}$ (mostly from 1 to $10^2\,\mu\mathrm{mol\,N\,m^{-2}\,d^{-1}}$; Fig. 8a). Some high rates (i.e., 10^2–$10^3\,\mu\mathrm{mol\,N\,m^{-2}\,d^{-1}}$) were found in the western Pacific Ocean, the regions near the Hawaiian Islands, and the western tropical Atlantic Ocean. Approximately 10 % of the depth-integrated N$_2$ fixation rates were $< 1\,\mu\mathrm{mol\,N\,m^{-2}\,d^{-1}}$ and were mainly from the North Atlantic and Indian oceans. Within the water column, the N$_2$ fixation rates were highest in the upper 25 m (Fig. 8b and c), below which the rates rapidly decreased with depth (Fig. 8d–f). In the upper 25 m, volumetric N$_2$ fixation rates in the southwestern Pacific were higher than those in other areas, mostly ranging from 1 to $100\,\mu\mathrm{mol\,N\,m^{-3}\,d^{-1}}$. Undetectable N$_2$ fixation rates were reported mostly in subpolar regions, as well as in certain tropical and subtropical regions (Fig. 8).
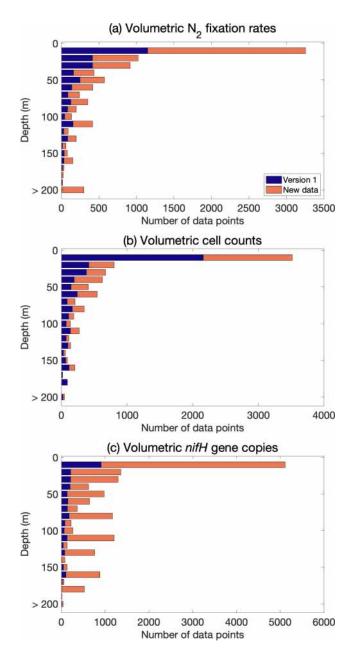
Figure 7. Vertical distribution number of **(a)** N$_2$ fixation rates, **(b)** cell abundance, and **(c)** *nifH* gene copy abundance data, including the data from version 1 of the database (blue) and the new data added to version 2 of the database (orange).

Cell-specific N$_2$ fixation rates span a range from 10^{-4} to 10^3 fmol N cell^{-1} d^{-1}, although mostly on the order of 10^{-2} to 10^2 fmol N cell^{-1} d^{-1} (Fig. 9). The mean cell-specific N$_2$ fixation rates of *Trichodesmium*, UCYN-A2, and heterocystous cyanobacteria were 1 to 2 orders of magnitude higher than those of other diazotrophic groups (Fig. 9 and Table S1).

3.3 Diazotrophic abundance

The depth-integrated cell abundances and volumetric cell abundances in the upper 25 m are also shown as the arithmetic means in 3° latitude × 3° longitude bins (Fig. 10). *Trichodesmium* abundance generally decreased from the west to the east in the Atlantic Ocean (Fig. 10a and b). In the Pacific Ocean, *Trichodesmium* appeared more abundant in the west. The abundance data of heterocystous diazotrophs were still scarce (Fig. 10c and e). The volumetric cell-count-based abundance data are also displayed in three additional depth intervals (Fig. S6).

Gene copies of *nifH* had better spatial coverage than the cell-count data (Fig. 11). Depth-integrated *Trichodesmium nifH* copies were also more abundant in the western Pacific and western Atlantic oceans (Fig. 11a). Some high depth-integrated *nifH* abundance of UCYN-A and UCYN-B were also reported in the northwestern and southwestern Pacific Ocean (Fig. 11c and e). High *nifH* abundances of *Richelia* were found in the southwestern Pacific Ocean and western Atlantic oceans (Fig. 11i). The *nifH* abundance data for UCYN-C and het-3 were sparse. The volumetric *nifH* abundance data are displayed in three depth intervals (Figs. 11 and S7). Almost all diazotrophs were more abundant in the upper 25 m than in deeper water.

3.4 First-order estimate of global oceanic N$_2$ fixation rate

Compared to version 1, the spatial coverage of data in version 2, in terms of the fraction of 3° latitude × 3° longitude bins, was greatly increased in all ocean basins (Table 8). The spatial data coverage was very low in the Southern and Arctic oceans (1 % and 2 % of total bins, respectively; Table 8), and we therefore did not estimate total N$_2$ fixation rates for these two basins. Please note that the inaccurate areas of the North and South Pacific oceans used in estimating the global oceanic N$_2$ fixation rate by Luo et al. (2012) was corrected in this study (Table 8).

We first compared the N$_2$ fixation rates estimated based on arithmetic means of version 1 and version 2 (Table 8). Using available data in version 2, the global N$_2$ fixation rate was determined to be 223 ± 30 Tg N yr^{-1}, which was 3 times that obtained from version 1 (Table 8). The substantial increase was mostly driven by notable changes in the South Pacific, North Atlantic, and Indian oceans. In the South Pacific Ocean, numerous high N$_2$ fixation rates were observed in the western subtropical region over the past decade (Fig. 12), resulting in a substantial increase of 68 ± 23 Tg N yr^{-1} in the estimated N$_2$ fixation rate for this basin (Table 8). It is worth noting that these newly recorded measurements in the western subtropics of the South Pacific Ocean might even be underestimated since most of them were obtained using the original ^{15}N$_2$ bubble method. In the North Atlantic Ocean, the estimated N$_2$ fixation rate also experienced an increase
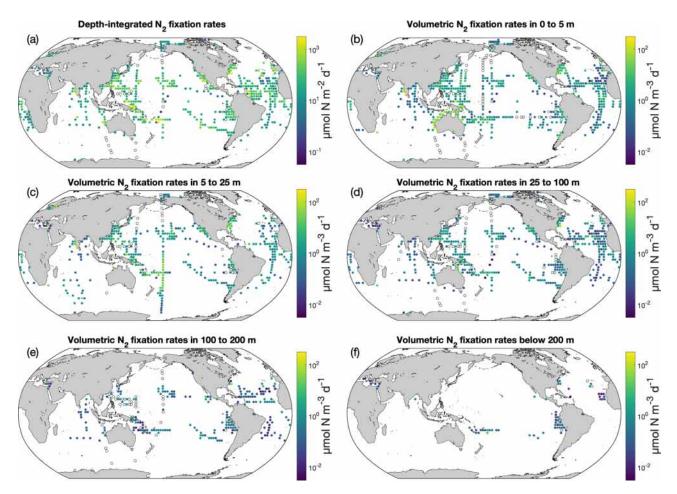
Figure 8. N₂ fixation rates in version 2 of the database. The panels show **(a)** depth-integrated data and volumetric data at **(b)** 0–5 m, **(c)** 5–25 m, **(d)** 25–100 m, **(e)** 100–200 m, and **(f)** below 200 m. For a clear demonstration, arithmetic mean N₂ fixation rates in 3° latitude × 3° longitude bins are shown. Zero-value data are denoted as black empty circles. Only rates measured with incubation periods of 24 h are included.

Table 8. First-order estimates of N₂ fixation rates based on their arithmetic means in different ocean basins. Data are first binned to 3° latitude × 3° longitude grids before being used to calculate arithmetic means in each basin. The arithmetic means are multiplied by the basin areas to calculate the N₂ fixation rates of each basin. NQ: not quantified due to limited data points. ND: no data. The values in the parentheses are the percentages of 3° × 3° bins in each basin that have measurements. The reported uncertainties are one standard error of the mean.

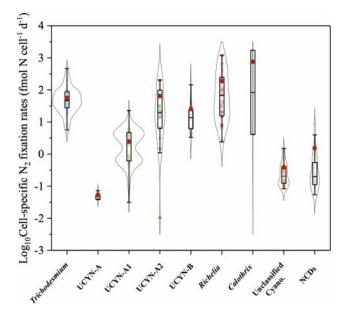| Region	Number of binned data		Latitudinal range		Ocean area ($\times 10^{12}\,\mathrm{m}^2$)		Arithmetic mean N₂ fixation rate ($\mu\mathrm{mol\,N\,m}^{-2}\,\mathrm{d}^{-1}$)		Areal sum of N₂ fixation rate ($\mathrm{Tg\,N\,yr}^{-1}$)	
	version 1	version 2	version 1	version 2	version 1	version 2	version 1	version 2	version 1	version 2
North Atlantic	47 (9 %)	116 (21 %)	0°–55° N	0°–55° N	37	37	55 ± 9	213 ± 46	10 ± 2	40 ± 9
South Atlantic	14 (4 %)	52 (15 %)	40° S–0°	45° S–0°	26	30	13 ± 4	30 ± 5	1.8 ± 0.6	5 ± 1
North Pacific	34 (4 %)	143 (17 %)	0°–55° N	0°–55° N	75	75	111 ± 17	144 ± 28	42 ± 7	55 ± 11
South Pacific	20 (2 %)	100 (12 %)	40° S–0°	45° S–0°	63	69	61 ± 7	250 ± 66	20 ± 2	88 ± 23
Indian Ocean	ND	47 (9 %)		45° S–25° N		56	ND	123 ± 50	ND	35 ± 14
Mediterranean Sea	1 (3 %)	9 (23 %)	30–45° N	30–45° N	2.5	2.5	NQ	5 ± 1	NQ	0.06 ± 0.02
Arctic Ocean	ND	17 (2 %)				11	ND	23 ± 5	ND	NQ
Southern Ocean	ND	10 (1 %)				60	ND	9 ± 8	ND	NQ
Global Ocean									74 ± 7	223 ± 30

Figure 9. Violin plot of cell-specific N$_2$ fixation rates, including measurements for *Trichodesmium*, UCYN-A, UCYN-A1, UCYN-A2, UCYN-B, heterocystous cyanobacteria, unclassified cyanobacteria, and NCDs. The range of each box spans the 25th–75th percentile of data, the black line in each box is the median, and the red dot represents the arithmetic mean.

of 30 ± 9 Tg N yr^{-1} for (Table 8), without any discernible pattern regarding the locations of the new high N$_2$ fixation measurements (Fig. 13). Furthermore, in the Indian Ocean, the improved data coverage in version 2 (Fig. 8a) supported the estimation of an N$_2$ fixation rate of 35 ± 14 Tg N yr^{-1} for this basin (Table 8), which was not possible to calculate using version 1 due to insufficient data availability.

However, when estimating the global marine N$_2$ fixation rate using geometric means, both version 1 and version 2 yielded similar rates of approximately 50 Tg N yr^{-1} (Table 9). The N$_2$ fixation rates in each basin tended to follow a log-normal distribution (Fig. 14), with the geometric mean aligning near the peak of the distribution. In the South Pacific Ocean, as discussed earlier, version 2 included a substantial number of newly observed high N$_2$ fixation rates, but it also incorporated a significant number of rates that were much lower than those in version 1 (Fig. 14c). This could be partially attributed to enhanced detection limits in measurements. Consequently, while version 2 yielded a much higher arithmetic mean N$_2$ fixation rate compared to version 1 for the South Pacific Ocean (Table 8), their geometric means remained quite similar (Table 9). In the North Pacific Ocean, for the same reasons, the arithmetic mean N$_2$ fixation rates obtained from both versions were very close, while the geometric mean of version 1 was even higher than that of version 2 (Tables 8 and 9; Fig. 14a). These analyses reveal that, despite the similarity in geometric means of N$_2$ fixation rates obtained from both versions of the database, the higher arith-

metic means in version 2 were not coincidental. Instead, they were the direct outcome of the improved measurement methods and the expanded spatial and temporal coverage of marine N$_2$ fixation over the past decade. Consequently, previous assessments of the global marine N$_2$ fixation rate were likely underestimated due to the absence of these new measurements.

We must emphasize that this calculation simply used the average N$_2$ fixation rates in different ocean basins; therefore, our calculation can only be considered a first-order estimate. Furthermore, limited measurements have shown a large range of N$_2$ fixation rates in the Southern Ocean (Fig. 8). Considering its vast area, future measurements expanding coverage of N$_2$ fixation rates in the Southern Ocean (see White et al., 2022) may help to better constrain the contribution of N$_2$ fixation to the N budget of the global ocean. The new database presented here also expands opportunities for improved statistical estimates of N$_2$ fixation patterns and global rates based on the modeling of environmental controls (Luo et al., 2014).

4 Discussion

4.1 Comparison of N$_2$ fixation measured using ^{15}N$_2$ bubble and dissolution methods

To date, the origin of the discrepancy in the N$_2$ fixation rates estimated using different ^{15}N$_2$ tracer methods remains unclear. As shown above, the volumetric N$_2$ fixation rates obtained by the original ^{15}N$_2$ bubble method and the ^{15}N$_2$ dissolution method spanned a similar range (Fig. 1), while the average rates using the former method were significantly lower than that measured using the latter method (one-tailed Wilcoxon test, $p < 0.001$, $n = 2460$ and 1128). With substantial data accumulated over the past decade, we further compared N$_2$ fixation rates measured using the two methods at close locations and sampling time, although the samples were not identical. We first binned data collected from the same months, horizontal locations ($3°$ latitude $\times$ $3°$ longitude), and depth intervals (0–5, 5–25, 25–100, and 100–200 m) and calculated the average rates for each method in each bin. The results showed that the original ^{15}N$_2$ bubble method produced lower rates than the ^{15}N$_2$ dissolution method in 69 % of the cases (Fig. 13). Furthermore, our analysis employing the generalized additive model (GAM) revealed that the relationship between the rates measured using the original ^{15}N$_2$ bubble method and those obtained through the ^{15}N$_2$ dissolution method closely adhered to the 1 : 1 line, albeit with slightly lower values in the former (Fig. 15). Please note that these slightly lower values can still result in significant underestimation in measured N$_2$ fixation rates because the GAM model was applied in a logarithmic space. It is crucial to reiterate that the rates being compared were derived from different samples, emphasizing the necessity for future investigations that directly compare the two methods
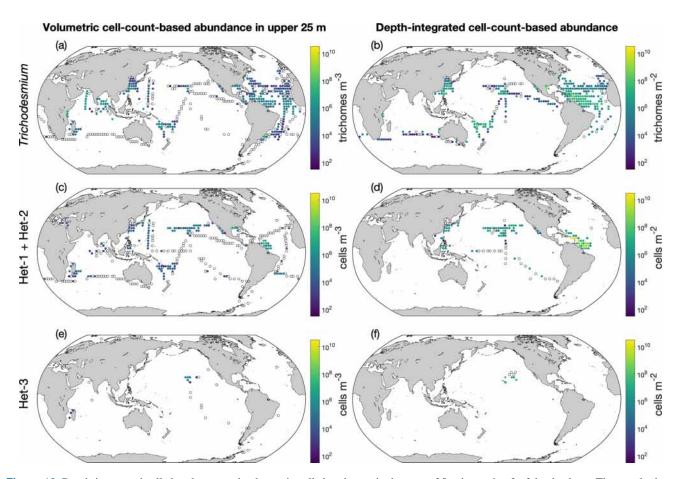
Figure 10. Depth-integrated cell abundances and volumetric cell abundances in the upper 25 m in version 2 of the database. The panels show **(a, b)** *Trichodesmium*, **(c, d)** het-1/2, and **(e, f)** het-3. For a clear demonstration, data are binned to 3° latitude × 3° longitude, and arithmetic means in each bin are shown. Zero-value data are denoted as open black circles.
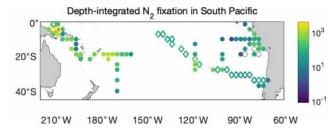
Table 9. Same as Table 8 but based on the geometric means of N$_2$ fixation rates. The numbers in parentheses are estimated ranges based on one standard error of log-transformed N$_2$ fixation rates (see Sect. 2.4).

Region	Proportion of zero-value data		Geometric mean N$_2$ fixation rate (μmol N m^{-2} d^{-1})		Areal sum of N$_2$ fixation rate (Tg N yr^{-1})	
	version 1	version 2	version 1	version 2	version 1	version 2
North Atlantic	0 %	5 %	22 (18–26)	46 (39–54)	4.1 (3.3–5.0)	8.7 (7.4–10.1)
South Atlantic	0 %	25 %	8 (6–10)	15 (13–17)	1.1 (0.9–1.3)	2.3 (1.9–2.7)
North Pacific	3 %	6 %	73 (63–83)	45 (39–52)	27.8 (24.2–32.0)	17.3 (15.1–19.8)
South Pacific	0 %	9 %	52 (45–59)	51 (43–61)	16.6 (14.4–19.1)	18.0 (15.1–21.4)
Indian Ocean	ND	0 %	ND	25 (20–31)	ND	7.1 (5.7–8.9)
Mediterranean Sea	0 %	3 %	NQ	3 (2–4)	NQ	0.04 (0.03–0.05)
Arctic Ocean	ND	2 %	ND	14 (11–18)	ND	NQ
Southern Ocean	ND	70 %	ND	4 (1–16)	ND	NQ
Global Ocean					50 (43–57)	53 (45–63)

Figure 11. Volumetric and depth-integrated *nifH* gene copy abundances in version 2 of the database. For volumetric abundances, only data in the upper 25 m are shown. The panels show gene copy abundances of **(a, b)** *Trichodesmium*, **(c, d)** UCYN-A, **(e, f)** UCYN-B, **(g, h)** UCYN-C, **(i, j)** het-1 + het-2, **(k, l)** het-3, and **(m, n)** Gamma A (an NCD phylotype). Depth-integrated data for Gamma A are not available. For a clear demonstration, data are binned to 3° latitude × 3° longitude and arithmetic means in each bin are shown. Zero-value data are denoted as open black circles.

Figure 12. Depth-integrated N$_2$ fixation rates in the South Pacific Ocean (μmol N m^{-2} d^{-1}). The shown data are arithmetic mean rates in 3° latitude × 3° longitude bins. Empty diamonds and filled circles denote the existing data in version 1 of the database and the new data added to version 2, respectively.

Figure 13. Depth-integrated N$_2$ fixation rates in the North Atlantic Ocean (μmol N m^{-2} d^{-1}). The shown data are arithmetic mean rates in 3° latitude × 3° longitude bins. Empty diamonds and filled circles denote the existing data in version 1 of the database and the new data added to version 2, respectively.

using the same samples with controlled parameters such as temperature, volume of injected ^{15}N$_2$, and incubation volume. Despite this limitation, our analysis suggests that the extensive body of historical marine N$_2$ fixation rate data obtained through the original ^{15}N$_2$ bubble method is still valuable, particularly in the examination of spatial and temporal variations in N$_2$ fixation.

We also used the same procedure to compare the N$_2$ fixation rates measured using acetylene reduction assays and the ^{15}N$_2$ tracer methods. However, there were insufficient pairs of data available for reliable comparisons ($n = 16$ for acetylene reduction versus the ^{15}N$_2$ dissolution method; $n = 6$ for acetylene reduction versus original ^{15}N$_2$ bubble method).

4.2 Comparison between diazotrophic cell counts and *nifH* copies

Whether or not *nifH* copies can be used to infer diazotrophic abundance and to study diazotrophic biogeography, some still challenges remain in the conversion of gene counts to biomass, as a large range in the number of *nifH* copies per diazotrophic cell has been re-

ported (Table S2). In version 2, we first converted *Trichodesmium* trichome abundance to cell abundance using the same conversion factor of 100 cells trichome^{-1} as that used in Luo et al. (2012). This conversion resulted in the mean and variance of log$_{10}$-transformed *Trichodesmium* cell abundance ($10^{6.5\pm1.3}$ cells L^{-1}) very similar to that those *Trichodesmium nifH* gene copies ($10^{6.6\pm1.5}$ copies L^{-1}; Fig. 16a). More recently, however, a much lower conversion factor of 13.2 ± 2.3 cells trichome^{-1} was suggested for *Trichodesmium* based on larger sample sizes, although a very large range of 1.2–685 cells trichome^{-1} was reported (White et al., 2018). Hence, when a conversion factor of 10 cells trichome^{-1} was applied, the *Trichodesmium nifH* gene copy abundance was 1 order of magnitude higher than its cell abundance (Fig. 16a). This result was within the reported mean *nifH* : cell ratios for *Trichodesmium*, albeit based on sparse samples, on the order of 10–100 (Table S2). It is worth noting that there have been suggestions that the observed *nifH* : cell ratio for *Trichodesmium* may be overestimated due to methodological limitations (Gradoville et al., 2022). Our analyses underscore the importance of enumerating *Trichodesmium* cells, rather than solely focusing on trichomes, in correctly evaluating *Trichodesmium* abundance, which has been suggested for future studies by White et al. (2018). While counting all *Trichodesmium* cells may be impractical, it would be valuable to report the number of cells in random samples of *Trichodesmium* trichomes.

The same analyses for heterocystous cyanobacteria showed that the *nifH* gene copy abundances were approximately 2 orders of magnitude greater than the cell abundances in terms of both mean and distribution (Fig. 16b and c). It must be noted that this simple analysis used all the data in our database. The limited in situ measurements for identical samples resulted in a mean *nifH* : cell ratio of 76 for heterocystous cyanobacteria (Table S2), consistent with our simple analysis.

In contrast, much lower *nifH* : cell ratios (1.51–2.58) were derived from regression analysis for heterocystous cyanobacteria and UCYN-B collected in the subtropical North Pacific (Gradoville et al., 2022). Considering these overall scarce measurements and the outcomes of our analysis, it is plausible that there is substantial variability in *nifH* : cell ratios. We expect that future studies, focusing on constraining these ratios and identifying mechanisms underlying variability in these ratios, will contribute to a more comprehensive understanding of the connection between *nifH* gene counts and diazotrophic cell abundance.

The application of qPCR assays for *nifH*-based abundance (DNA) and expression (RNA) has emerged as a critical step forward in our understanding of the distribution, abundance, and physiology (e.g., expression of *nifH*) of diazotrophs (Short and Zehr, 2005; Zehr and Riemann, 2023). Previously, estimating the abundances of diazotrophs was limited to those that could be identified by microscopy, e.g., *Trichodesmium*, heterocystous cyanobacteria (e.g., *Riche-*
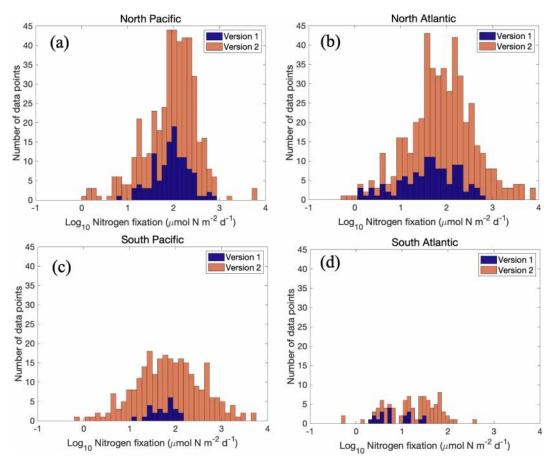
Figure 14. Comparison of the distribution of log-transformed N$_2$ fixation rates between the two versions of the database. Note that the zero-value data are not included because of the log transformation. The comparison is performed for data in **(a)** North Pacific, **(b)** North Atlantic, **(c)** South Pacific, and **(d)** South Atlantic oceans.

lia, *Calothrix*, *Anabaena*, *Nodularia*, *Aphanizomenon*), and some unicellulars (e.g., *Cyanothece*, later *Crocosphaera*). Thus, qPCR enabled the study of diazotrophic targets (and their activity) without the need for microscopy to identify them, which came later as some diazotrophs did (and still do) require application of FISH techniques for identification (Biegala and Raimbault, 2008). Additionally, qPCR allowed the study of in situ activity (gene expression) by diazotrophs without the need for cultivation. Although beyond the scope of the work presented here, important considerations should be taken into account when applying microscopy and qPCR datasets (Table S3), for example, to biogeochemical models (Meiler et al., 2023).

4.3 Biomass conversion factor

For possible further usage of cell-counted abundance data, here we suggest carbon biomass conversion factors for different diazotrophic groups (Tables 10 and S4). Most biomass conversion factors suggested here are the same as those used in Luo et al. (2012), excluding UCYN-A and heterocystous cyanobacteria, where new information has become available

or additional consideration is necessary. A recent study has discovered a new symbiosis association between the unicellular diazotroph (UCYN-C) and diatom *Epithemia* strains (Schvarcz et al., 2022). However, the conversion factor of UCYN-C could not be updated in this study due to insufficient information on the biovolumes of host cell.

The conversion factor for UCYN-A was updated because it has been found to live symbiotically with haptophyte *Braarudosphaera bigelowii* and relatives (Thompson et al., 2012; Hagino et al., 2013). Because the host and UCYN-A should function together, the host biomass is allocated to UCYN-A. It has been reported that each haptophyte cell hosts one UCYN-A1 cell (Cornejo-Castillo et al., 2019) or one UCYN-A2 cell (Suzuki et al., 2021). We used the empirically derived equation (Verity et al., 1992)

$$C = 0.433 \times V^{0.863} \tag{1}$$

to estimate the biomass of UCYN-A and their hosts. The biomasses of a UCYN-A1 cell with a diameter of 1 μm and a UCYN-A2 cell with a diameter of 1.6–3.3 μm (Cornejo-Castillo et al., 2019; Martínez-Pérez et al., 2016) are 0.2 and
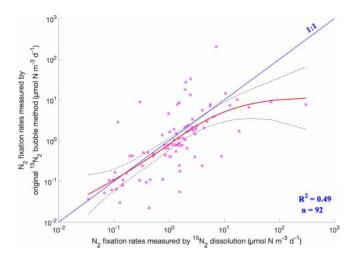
Figure 15. Comparison of measured N$_2$ fixation rates using the original ^{15}N$_2$ bubble method and the ^{15}N$_2$ dissolution method. The pink dots are measurements. The fitted results of the two methods by the generalized additive model (GAM) and confidence intervals are represented by the red solid line and the dashed black lines, respectively. Only the N$_2$ fixation rates measured with incubation periods of 24 h were included in this analysis.

0.8–5.5 pg C, respectively. The biomasses of the host cell for UCYN-A1 or UCYN-A2 is 1.5–2.2 or 6.8–43 pg C according to their reported cell diameters (2–2.3 or 3.6–7.3 μm), respectively (Martínez-Pérez et al., 2016; Cornejo-Castillo et al., 2019). Hence, the biomasses of the UCYN-A1 and the UCYN-A2 symbioses are 1.7–2.4 and 7.6–48 pg C, respectively. After normalizing the symbiotic biomass to the number of UCYN cells in each symbiosis (1 for both UCYN-A1 and UCYN-A2), the biomass conversion factors are 1.7–2.4 pg C (UCYN-A1 cell)$^{-1}$ and 7.6–48 pg C (UCYN-A2 cell)$^{-1}$.

Because heterocystous cyanobacteria and their host diatoms form DDAs, similar to UCYN-A, we also suggest allocating the biomass of host diatoms to each associated diazotrophic cell (Table S4). The biomasses of heterocystous cells and vegetative cells in *Richelia* filaments were updated according to the cell dimension data reported in Caputo et al. (2019) using the same empirical equation above. The carbon biomass of host diatom cells was calculated using an empirical equation (Menden-Deuer and Lessard, 2000):

$$C = 0.117 \times V^{0.881}, \tag{2}$$

where C is the diatom cell carbon biomass (pg C cell^{-1}) and V is the average cell biovolume (μm^3) of each diatom genus, for which values from a database (Harrison et al., 2015) were used in this study (Table S4). Each host diatom associates with multiple heterocysts. The numbers of *Richelia* heterocysts associated with *Hemiaulus*, *Rhizosolenia*, and *Chaetoceros* were observed to be within the range of 1–2, 1–5, and 3–10 respectively (Villareal et al., 2011; Yeung et al., 2012; Caputo et al., 2019); we selected both the maximum and min-

imum to do the estimation. The number of vegetative cells in each heterocyst was also updated according to Caputo et al. (2019). Conversion factors for DDAs were estimated by dividing the total biomass of each DDA by the number of associated heterocysts. Changes in the number of *Richelia* in *Rhizosolenia* (1 or 5) would make a large variation in its conversion factor, possibly due to the large host biomass; therefore, we keep them both to let users take caution when using this conversion factor. The resulting biomass conversion factors of *Richelia–Hemiaulus* and *Richelia–Chaetoceros* associations were estimated to be 280 pg C heterocyst^{-1} (range: 150–1250) and 430 pg C heterocyst^{-1} (range: 10–1900), respectively (Table S4), as the number of filaments did not have a large impact on the conversion factors.

It is important to reiterate that these biomass conversion factors are only applicable to cell-count data. Attempting to convert *nifH* gene copies to biomass is not recommended due to significant uncertainties associated with *nifH* : cell ratios, as previously discussed.

5 Data availability

The database is available in a data repository (https://doi.org/10.6084/m9.figshare.21677687, Shao et al., 2022).

6 Conclusions

In this study, we updated the global oceanic diazotrophic database by Luo et al. (2012) by adding new measurements reported in the past decade. Although the spatial coverage of the data was greatly expanded by this effort, the data distribution is still uneven, with most measurements reported from the Pacific and Atlantic oceans. Using the updated database, the estimation of global oceanic N$_2$ fixation based on arithmetic rates in ocean basins was increased from 74 ± 7 to 223 ± 30 Tg N yr^{-1}. This change is largely attributable to a new estimate for the Indian Ocean and a much elevated estimate for the South Pacific Ocean, the latter of which would account for $\sim 40\%$ of global N$_2$ fixation. This high estimation for the South Pacific Ocean is in line with its qualification as a hotspot for diazotrophy (Messer et al., 2016; Bonnet et al., 2017), partly due to iron fertilization processes in this region (Bonnet et al., 2023). Due to data sparsity, our updated estimation did not include N$_2$ fixation in the Southern and Arctic oceans. Furthermore, data were more concentrated in surface seawater, and a significant amount of data were measured with incubation periods shorter than a daily cycle (24 h), limiting reliable evaluations of depth-integrated N$_2$ fixation rates. Although this result suggests more balanced N inputs and losses in the global ocean than the previous estimate suggested, large uncertainties still exist. We also compared the N$_2$ fixation rates measured using the addition of a bubble of labeled gas or the addition of dissolving
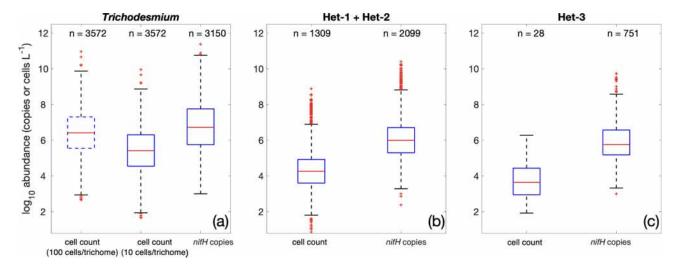
Figure 16. Comparison of all cell-count and *nifH* gene copy abundance data in the database. The box plots show the median (central line), 25th and 75th percentiles (upper and lower edges of the boxes), 5th and 95th percentiles (error lines), and outliers (red crosses) of the log$_{10}$-transformed data. The comparisons are conducted for **(a)** *Trichodesmium*, **(b)** het-1/2, and **(c)** het-3. Note that the two conversion factors of 10 and 100 cells trichome^{-1} are used for *Trichodesmium*.

Table 10. Recommended carbon biomass conversion factors and their likely ranges for diazotrophic groups.

	Trichodesmium (pg C cell^{-1})	UCYN-A1 (pg C cell^{-1})	UCYN-A2 (pg C cell^{-1})	UCYN-B (pg C cell^{-1})	UCYN-C (pg C cell^{-1})	Het-1 *Richelia–Hemiaulus* (pg C heterocyst^{-1})	Het-2 *Richelia–Rhizosolenia* (pg C heterocyst^{-1})	Het-3 *Richelia–Chaetoceros* (pg C heterocyst^{-1})
Recommended	300	2	30	20	10	350	450 (5 heterocyst DDA^{-1}) or 1900 (1 heterocyst DDA^{-1})	50
Likely range	100–500	1–3	10–50	4–50	5–24	150–1030	19–5700	9–300

^{15}N$_2$ gases reported at the same location and month (not necessarily in identical samples). The results indicated that the original ^{15}N$_2$ bubble method produces lower rates than the ^{15}N$_2$ dissolution method in 69 % of the cases. These results reveal that, despite decades of effort, the ocean is still undersampled in terms of the distribution of diazotrophs and N$_2$ fixation rate measurements. Our analyses suggest that prioritizing N$_2$ fixation measurements in the South Pacific Ocean, Indian Ocean, and high northern latitudes can significantly reduce the current uncertainty of N$_2$ fixation rates in the global ocean. Nevertheless, we believe that this updated diazotrophic database, supplemented with enhanced data from the past decade, is timely and can be helpful to scientists studying the marine biogeochemical cycle of N.

Review statement. This paper was edited by Xingchen Wang and reviewed by Christopher Somes and one anonymous referee.

References

Agawin, N. S. R., Tovar-Sánchez, A., De Zarruk, K. K., Duarte, C. M., and Agustí, S.: Variability in the abundance of *Trichodesmium* and nitrogen fixation activities in the subtropical NE Atlantic, J. Plankton Res., 35, 1126–1140, https://doi.org/10.1093/plankt/fbt059, 2013.

Ahmed, A., Gauns, M., Kurian, S., Bardhan, P., Pratihary, A., Naik, H., Shenoy, D. M., and Naqvi, S. W. A.: Nitrogen fixation rates in the eastern Arabian Sea, Estuarine, Coast. Shelf Sci., 191, 74–83, https://doi.org/10.1016/j.ecss.2017.04.005, 2017.

Barthel, K.-G., Schneider, G., Gradinger, R., and Lenz, J.: Concentration of live pico- and nanoplankton by means of tangential flow filtration, J. Plankton Res., 11, 1213–1221, https://doi.org/10.1093/plankt/11.6.1213, 1989.

Benavides, M., Agawin, N. S. R., Arístegui, J., Peene, J., and Stal, L. J.: Dissolved organic nitrogen and carbon release by a marine unicellular diazotrophic cyanobacterium, Aquat. Microb. Ecol., 69, 69–80, https://doi.org/10.3354/ame01621 2013a.

Benavides, M., Bronk, D. A., Agawin, N. S. R., Pérez-Hernández, M. D., Hernández-Guerra, A., and Arístegui, J.: Longitudinal variability of size-fractionated N₂ fixation and DON release rates along 24.5° N in the subtropical North Atlantic, J. Geophys. Res.-Oceans, 118, 3406–3415, https://doi.org/10.1002/jgrc.20253, 2013b.

Benavides, M., Santana-Falcón, Y., Wasmund, N., and Aristegui, J.: Microbial uptake and regeneration of inorganic nitrogen off the coastal Namibian upwelling system, J. Marine Syst., https://doi.org/10.1016/j.jmarsys.2014.05.002, 2014.

Benavides, M., Moisander, P. H., Berthelot, H., Dittmar, T., Grosso, O., and Bonnet, S.: Mesopelagic N₂ fixation related to organic matter composition in the Solomon and Bismarck Seas (Southwest Pacific), Plos One, 10, 12, https://doi.org/10.1371/journal.pone.0143775, 2015.

Benavides, M., Bonnet, S., Hernandez, N., Martinez-Perez, A. M., Nieto-Cid, M., Alvarez-Salgado, X. A., Banos, I., Montero, M. F., Mazuecos, I. P., Gasol, J. M., Osterholz, H., Dittmar, T., Berman-Frank, I., and Aristegui, J.: Basin-wide N₂ fixation in the deep waters of the Mediterranean Sea, Global Biogeochem. Cycles, 30, 952–961, https://doi.org/10.1002/2015gb005326, 2016a.

Benavides, M., Moisander, P. H., Daley, M. C., Bode, A., and Aristegui, J.: Longitudinal variability of diazotroph abundances in the subtropical North Atlantic Ocean, J. Plankton Res., 38, 662–672, https://doi.org/10.1093/plankt/fbv121, 2016b.

Benavides, M., Berthelot, H., Duhamel, S., Raimbault, P., and Bonnet, S.: Dissolved organic matter uptake by *Trichodesmium* in the Southwest Pacific, Sci. Rep.-UK, 7, 41315, https://doi.org/10.1038/srep41315, 2017.

Benavides, M., Bonnet, S., Berman-Frank, I., and Riemann, L.: Deep into oceanic N₂ fixation, Front. Marine Sci., 5, 108, https://doi.org/10.3389/fmars.2018.00108, 2018a.

Benavides, M., Shoemaker, K. M., Moisander, P. H., Niggemann, J., Dittmar, T., Duhamel, S., Grosso, O., Pujo-Pay, M., Hélias-Nunige, S., Fumenia, A., and Bonnet, S.: Aphotic N₂ fixation along an oligotrophic to ultraoligotrophic transect in the western tropical South Pacific Ocean, Biogeosciences, 15, 3107–3119, https://doi.org/10.5194/bg-15-3107-2018, 2018b.

Benavides, M., Conradt, L., Bonnet, S., Berman-Frank, I., Barrillon, S., Petrenko, A., and Doglioli, A.: Fine-scale sampling unveils diazotroph patchiness in the South Pacific Ocean, ISME Commun., 1, 3, https://doi.org/10.1038/s43705-021-00006-2, 2021.

Benavides, M., Bonnet, S., Le Moigne, F. A. C., Armin, G., Inomura, K., Hallstrøm, S., Riemann, L., Berman-Frank, I., Poletti, E., Garel, M., Grosso, O., Leblanc, K., Guigue, C., Tedetti, M., and Dupouy, C.: Sinking *Trichodesmium* fixes nitrogen in the dark ocean, ISME J., 16, 2398–2405, https://doi.org/10.1038/s41396-022-01289-6, 2022a.

Benavides, M., Caffin, M., Duhamel, S., Foster, R. A., Grosso, O., Guieu, C., Van Wambeke, F., and Bonnet, S.: Anomalously high abundance of *Crocosphaera* in the South Pacific Gyre, FEMS Microbiol. Lett., 369, fnac039, https://doi.org/10.1093/femsle/fnac039, 2022b.

Bentzon-Tilia, M., Severin, I., Hansen, L. H., and Riemann, L.: Genomics and Ecophysiology of Heterotrophic Nitrogen-Fixing Bacteria Isolated from Estuarine Surface Water, mBio, 6, e00929-15, https://doi.org/10.1128/mbio.00929-15, 2015a.

Bentzon-Tilia, M., Traving, S. J., Mantikci, M., Knudsen-Leerbeck, H., Hansen, J. L., Markager, S., and Riemann, L.: Significant N₂ fixation by heterotrophs, photoheterotrophs and heterocystous cyanobacteria in two temperate estuaries, ISME J., 9, 273–285, https://doi.org/10.1038/ismej.2014.119, 2015b.

Berthelot, H., Bonnet, S., Camps, M., Grosso, O., and Moutin, T.: Assessment of the dinitrogen released as ammonium and dissolved organic nitrogen by unicellular and filamentous marine diazotrophic cyanobacteria grown in culture, Front. Mar. Sci., 2, 80, https://doi.org/10.3389/fmars.2015.00080, 2015.

Berthelot, H., Benavides, M., Moisander, P. H., Grosso, O., and Bonnet, S.: High-nitrogen fixation rates in the particulate and dissolved pools in the Western Tropical Pacific (Solomon and Bismarck Seas), Geophys. Res. Lett., 44, 8414–8423, https://doi.org/10.1002/2017gl073856, 2017.

Berthelot, H., Duhamel, S., L'Helguen, S., Maguer, J.-F., Wang, S., Cetiniæ, I., and Cassar, N.: NanoSIMS single cell analyses reveal the contrasting nitrogen sources for small phytoplankton, ISME J., 13, 651–662, https://doi.org/10.1038/s41396-018-0285-8, 2019.

Bhavya, P. S., Kumar, S., Gupta, G. V. M., Sudheesh, V., Sudharma, K. V., Varrier, D. S., Dhanya, K. R., and Saravanane, N.: Nitrogen uptake dynamics in a tropical eutrophic estuary (Cochin, India) and adjacent coastal waters, Estuar. Coasts, 39, 54–67, https://doi.org/10.1007/s12237-015-9982-y, 2016.

Biegala, I. and Raimbault, P.: High abundance of diazotrophic picocyanobacteria ($< 3\,\mu$m) in a Southwest Pacific coral lagoon, Aquat. Microb. Ecol., 51, 45–53, https://doi.org/10.3354/ame01185, 2008.

Bif, M. and Yunes, J.: Distribution of the marine cyanobacteria *Trichodesmium* and their association with iron-rich particles in

the South Atlantic Ocean, Aquat. Microb. Ecol., 78, 107–119, https://doi.org/10.3354/ame01810, 2017.

Bird, C., Martinez, M. J., O'Donnell, A. G., and Wyman, M.: Spatial distribution and transcriptional activity of an uncultured clade of planktonic diazotrophic ã-proteobacteria in the Arabian Sea, Appl. Environ. Microbiol., 71, 2079–2085, https://doi.org/10.1128/AEM.71.4.2079-2085.2005, 2005.

Blais, M., Tremblay, J. É., Jungblut, A. D., Gagnon, J., Martin, J., Thaler, M., and Lovejoy, C.: Nitrogen fixation and identification of potential diazotrophs in the Canadian Arctic, Global Biogeochem. Cycles, 26, 1–13, https://doi.org/10.1029/2011gb004096, 2012.

Bombar, D., Moisander, P. H., Dippner, J. W., Foster, R. A., Voss, M., Karfeld, B., and Zehr, J. P.: Distribution of diazotrophic microorganisms and *nifH* gene expression in the Mekong River plume during intermonsoon, Mar. Ecol. Prog. Ser., 424, 39–55, https://doi.org/10.3354/meps08976, 2011.

Bombar, D., Taylor, C. D., Wilson, S. T., Robidart, J. C., Rabines, A., Turk-Kubo, K. A., Kemp, J. N., Karl, D. M., and Zehr, J. P.: Measurements of nitrogen fixation in the oligotrophic North Pacific Subtropical Gyre using a free-drifting submersible incubation device, J. Plankton Res., 37, 727–739, https://doi.org/10.1093/plankt/fbv049, 2015.

Bombar, D., Paerl, R. W., and Riemann, L.: Marine non-cyanobacterial diazotrophs: moving beyond molecular detection, Trends Microbiol., 24, 916–927, https://doi.org/10.1016/j.tim.2016.07.002, 2016.

Bonnet, S., Dekaezemacker, J., Turk-Kubo, K. A., Moutin, T., Hamersley, R. M., Grosso, O., Zehr, J. P., and Capone, D. G.: Aphotic N₂ Fixation in the Eastern Tropical South Pacific Ocean, PLoS ONE, 8, e81265, https://doi.org/10.1371/journal.pone.0081265, 2013.

Bonnet, S., Rodier, M., Turk-Kubo, K. A., Germineaud, C., Menkes, C., Ganachaud, A., Cravatte, S., Raimbault, P., Campbell, E., Quéroué, F., Sarthou, G., Desnues, A., Maes, C., and Eldin, G.: Contrasted geographical distribution of N₂ fixation rates and *nifH* phylotypes in the Coral and Solomon Seas (southwestern Pacific) during austral winter conditions, Global Biogeochem. Cycles, 29, 1874–1892, https://doi.org/10.1002/2015gb005117, 2015.

Bonnet, S., Caffin, M., Berthelot, H., and Moutin, T.: Hot spot of N₂ fixation in the western tropical South Pacific pleads for a spatial decoupling between N₂ fixation and denitrification, P. Natl. Acad. Sci. USA, 114, E2800–E2801, https://doi.org/10.1073/pnas.1619514114, 2017.

Bonnet, S., Caffin, M., Berthelot, H., Grosso, O., Benavides, M., Helias-Nunige, S., Guieu, C., Stenegren, M., and Foster, R. A.: In-depth characterization of diazotroph activity across the western tropical South Pacific hotspot of N₂ fixation (OUTPACE cruise), Biogeosciences, 15, 4215–4232, https://doi.org/10.5194/bg-15-4215-2018, 2018.

Bonnet, S., Guieu, C., Taillandier, V., Boulart, C., Bouruet-Aubertot, P., Gazeau, F., Scalabrin, C., Bressac, M., Knapp, A., Cuypers, Y., González-Santana, D., Forrer, H., Grisoni, J. M., Grosso, O., Habasque, J., Jardin-Camps, M., Leblond, N., Le Moigne, F., Lebourges-Dhaussy, A., and Tilliette, C.: Natural iron fertilization by shallow hydrothermal sources fuels diazotroph blooms in the ocean, Science, 380, 812–817, https://doi.org/10.1126/science.abq4654, 2023.

Böttjer, D., Dore, J. E., Karl, D. M., Letelier, R. M., Mahaffey, C., Wilson, S. T., Zehr, J., and Church, M. J.: Temporal variability of nitrogen fixation and particulate nitrogen export at Station ALOHA, Limnol. Oceanogr., 62, 200–216, https://doi.org/10.1002/lno.10386, 2017.

Breitbarth, E., Mills, M. M., Friedrichs, G., and LaRoche, J.: The Bunsen gas solubility coefficient of ethylene as a function of temperature and salinity and its importance for nitrogen fixation assays, Limnol. Oceanogr.-Methods, 2, 282–288, https://doi.org/10.4319/lom.2004.2.282, 2004.

Cabello, A. M., Turk-Kubo, K. A., Hayashi, K., Jacobs, L., Kudela, R. M., and Zehr, J. P.: Unexpected presence of the nitrogen-fixing symbiotic cyanobacterium UCYN-A in Monterey Bay, California, J. Phycol., 56, 1521–1533, https://doi.org/10.1111/jpy.13045, 2020.

Campbell, L., Carpenter, E., Montoya, J., Kustka, A., and Capone, D.: Picoplankton community structure within and outside a Trichodesmium bloom in the southwestern Pacific Ocean, Vie Milieu, 55, 185–195, 2005.

Capone, D. G.: Determination of nitrogenase activity in aquatic samples using the acetylene reduction procedure, in: Handbook of Methods in Aquat. Microb. Ecol., edited by: Kemp, P. F., Cole, J. J., Sherr, B. F., and Sherr, E. B., Lewis Publishers, Boca Raton, FL, 621–631, 1993.

Capone, D. G. and Montoya, J. P.: Nitrogen fixation and denitrification, Meth. Microbiol., 30, 501–515, https://doi.org/10.1016/S0580-9517(01)30060-0, 2001.

Capone, D. G., Burns, J. A., Montoya, J. P., Subramaniam, A., Mahaffey, C., Gunderson, T., Michaels, A. F., and Carpenter, E. J.: Nitrogen fixation by *Trichodesmium* spp.: An important source of new nitrogen to the tropical and subtropical North Atlantic Ocean, Global Biogeochem. Cycles, 19, GB2024, https://doi.org/10.1029/2004GB002331, 2005.

Caputo, A., Nylander, J. A. A., and Foster, R. A.: The genetic diversity and evolution of diatom-diazotroph associations highlights traits favoring symbiont integration (vol. 366, fny297, 2019), Fems Microbiol. Lett., 366, fny297, https://doi.org/10.1093/femsle/fnz120, 2019.

Cassar, N., Tang, W., Gabathuler, H., and Huang, K.: Method for High Frequency Underway N₂ Fixation Measurements: Flow-Through Incubation Acetylene Reduction Assays by Cavity Ring Down Laser Absorption Spectroscopy (FARACAS), Anal. Chem., 90, 2839–2851, https://doi.org/10.1021/acs.analchem.7b04977, 2018.

Cerdan-Garcia, E., Baylay, A., Polyviou, D., Woodward, E. M. S., Wrightson, L., Mahaffey, C., Lohan, M. C., Moore, C. M., Bibby, T. S., and Robidart, J. C.: Transcriptional responses of Trichodesmium to natural inverse gradients of Fe and P availability, ISME J., 16, 1055–1064, https://doi.org/10.1038/s41396-021-01151-1, 2021.

Chang, B. X., Jayakumar, A., Widner, B., Bernhardt, P., Mordy, C. W., Mulholland, M. R., and Ward, B. B.: Low rates of dinitrogen fixation in the eastern tropical South Pacific, Limnol. Oceanogr., 64, 1913–1923, https://doi.org/10.1002/lno.11159, 2019.

Chen, L. Y.-L., Chen, H.-Y., Lin, Y.-H., Yong, T.-C., Taniuchi, Y., and Tuo, S.-H.: The relative contributions of unicellular and filamentous diazotrophs to N₂ fixation in the South China Sea and the upstream Kuroshio, Deep-Sea Res. Pt. I, 85, 56–71, https://doi.org/10.1016/j.dsr.2013.11.006, 2014.

Chen, M. M., Lu, Y. Y., Jiao, N. Z., Tian, J. W., Kao, S. J., and Zhang, Y.: Biogeographic drivers of diazotrophs in the western Pacific Ocean, Limnol. Oceanogr., 64, 1403–1421, https://doi.org/10.1002/lno.11123, 2019.

Cheung, S., Liu, K., Turk-Kubo, K. A., Nishioka, J., Suzuki, K., Landry, M. R., Zehr, J. P., Leung, S., Deng, L., and Liu, H.: High biomass turnover rates of endosymbiotic nitrogen-fixing cyanobacteria in the western Bering Sea, Limnol. Oceanogr. Lett., 7, 501–509, https://doi.org/10.1002/lol2.10267, 2022.

Cheung, S. Y., Nitanai, R., Tsurumoto, C., Endo, H., Nakaoka, S., Cheah, W., Lorda, J. F., Xia, X. M., Liu, H. B., and Suzuki, K.: Physical forcing controls the basin-scale occurrence of nitrogen-fixing organisms in the North Pacific Ocean, Global Biogeochem. Cycles, 34, 9, https://doi.org/10.1029/2019GB006452, 2020.

Church, M. J. and Zehr, J.: Time series measurements of *nifH* gene abundances for several cyanobacteria in the subtropical North Pacific Ocean, Zenodo [data set], https://doi.org/10.5281/zenodo.4728253, 2020.

Church, M. J., Jenkins, B. D., Karl, D. M., and Zehr, J. P.: Vertical distributions of nitrogen-fixing phylotypes at Stn ALOHA in the oligotrophic North Pacific Ocean, Aquat. Microb. Ecol., 38, 3–14, https://doi.org/10.3354/ame038003, 2005a.

Church, M. J., Short, C. M., Jenkins, B. D., Karl, D. M., and Zehr, J. P.: Temporal Patterns of Nitrogenase Gene (*nifH*) Expression in the Oligotrophic North Pacific Ocean, Appl. Environ. Microbiol., 71, 5362–5370, https://doi.org/10.1128/aem.71.9.5362-5370.2005, 2005b.

Church, M. J., Björkman, K. M., Karl, D. M., Saito, M. A., and Zehr, J. P.: Regional distributions of nitrogen-fixing bacteria in the Pacific Ocean, Limnol. Oceanogr., 53, 63–77, https://doi.org/10.4319/lo.2008.53.1.0063, 2008.

Confesor, K. A., Selden, C. R., Powell, K. E., Donahue, L. A., Mellett, T., Caprara, S., Knapp, A. N., Buck, K. N., and Chappell, P. D.: Defining the Realized Niche of the Two Major Clades of Trichodesmium: A Study on the West Florida Shelf, Front. Marine Sci., 9, 821655, https://doi.org/10.3389/fmars.2022.821655, 2022.

Cornejo-Castillo, F. M., Cabello, A. M., Salazar, G., Sánchez-Baracaldo, P., Lima-Mendez, G., Hingamp, P., Alberti, A., Sunagawa, S., Bork, P., de Vargas, C., Raes, J., Bowler, C., Wincker, P., Zehr, J. P., Gasol, J. M., Massana, R., and Acinas, S. G.: Cyanobacterial symbionts diverged in the late Cretaceous towards lineage-specific nitrogen fixation factories in single-celled phytoplankton, Nat. Commun., 7, 11071, https://doi.org/10.1038/ncomms11071, 2016.

Cornejo-Castillo, F. M., Munoz-Marin, M. D. C., Turk-Kubo, K. A., Royo-Llonch, M., Farnelid, H., Acinas, S. G., and Zehr, J. P.: UCYN-A3, a newly characterized open ocean sublineage of the symbiotic N₂-fixing cyanobacterium Candidatus Atelocyanobacterium thalassa, Environ. Microbiol., 21, 111–124, https://doi.org/10.1111/1462-2920.14429, 2019.

Dabundo, R., Lehmann, M. F., Treibergs, L., Tobias, C. R., Altabet, M. A., Moisander, P. H., and Granger, J.: The contamination of commercial ¹⁵N₂ gas stocks with ¹⁵N-labeled nitrate and ammonium and consequences for nitrogen fixation measurements, PLoS One, 9, e110335, https://doi.org/10.1371/journal.pone.0110335, 2014.

Dekaezemacker, J., Bonnet, S., Grosso, O., Moutin, T., Bressac, M., and Capone, D. G.: Evidence of active dinitrogen fixation in surface waters of the eastern tropical South Pacific during El Nino and La Nina events and evaluation of its potential nutrient controls, Global Biogeochem. Cycles, 27, 768–779, https://doi.org/10.1002/gbc.20063, 2013.

Delmont, T. O., Pierella Karlusich, J. J., Veseli, I., Fuessel, J., Eren, A. M., Foster, R. A., Bowler, C., Wincker, P., and Pelletier, E.: Heterotrophic bacterial diazotrophs are more abundant than their cyanobacterial counterparts in metagenomes covering most of the sunlit ocean, ISME J., 16, 927–936, https://doi.org/10.1038/s41396-021-01135-1, 2021.

Detoni, A. M. S., Ciotti, Á. M., Calil, P. H. R., Tavano, V. M., and Yunes, J. S.: *Trichodesmium* latitudinal distribution on the shelf break in the southwestern Atlantic Ocean during spring and autumn, Global Biogeochem. Cycles, 30, 1738–1753, https://doi.org/10.1002/2016gb005431, 2016.

Detoni, A. M. S., Subramaniam, A., Haley, S. T., Dyhrman, S. T., and Calil, P. H. R.: Cyanobacterial diazotroph distributions in the western South Atlantic, Front. Marine Sci., 9, 856643, https://doi.org/10.3389/fmars.2022.856643, 2022.

Deutsch, C., Sarmiento, J. L., Sigman, D. M., Gruber, N., and Dunne, J. P.: Spatial coupling of nitrogen inputs and losses in the ocean, Nature, 445, 163–167, https://doi.org/10.1038/nature05392, 2007.

Dugenne, M., Gradoville, M., Church, M., Wilson, S., Sheyn, U., Harke, M., Björkman, K., Hawco, N., Hynes, A., Ribalet, F., Karl, D., DeLong, E., Dyhrman, S., Armbrust, E., John, S., Eppley, J., Harding, K., Stewart, B., Cabello, A., and Zehr, J.: Nitrogen Fixation in Mesoscale Eddies of the North Pacific Subtropical Gyre: Patterns and Mechanisms, Global Biogeochem. Cycles, 37, e2022GB00738, https://doi.org/10.1029/2022GB007386, 2023.

Dupouy, C., Benielli-Gary, D., Neveux, J., Dandonneau, Y., and Westberry, T. K.: An algorithm for detecting *Trichodesmium* surface blooms in the South Western Tropical Pacific, Biogeosciences, 8, 3631–3647, https://doi.org/10.5194/bg-8-3631-2011, 2011.

Estrada, M., Delgado, M., Blasco, D., Latasa, M., Cabello, A. M., Benítez-Barrios, V., Fraile-Nuez, E., Mozetiè, P., and Vidal, M.: Phytoplankton across tropical and subtropical regions of the Atlantic, Indian and Pacific oceans, PLoS One, 11, e0151699, https://doi.org/10.1371/journal.pone.0151699, 2016.

Farnelid, H., Bentzon-Tilia, M., Andersson, A. F., Bertilsson, S., Jost, G., Labrenz, M., Jürgens, K., and Riemann, L.: Active nitrogen-fixing heterotrophic bacteria at and below the chemocline of the central Baltic Sea, ISME J., 7, 1413–1423, https://doi.org/10.1038/ismej.2013.26, 2013.

Farnelid, H., Turk-Kubo, K., Muñoz-Marín, M. C., and Zehr, J. P.: New insights into the ecology of the globally significant uncultured nitrogen-fixing symbiont UCYN-A, Aquat. Microb. Ecol., 77, 125–138, https://doi.org/10.3354/ame01794, 2016.

Fernández, A., Mouriño-Carballido, B., Bode, A., Varela, M., and Marañón, E.: Latitudinal distribution of *Trichodesmium* spp. and N₂ fixation in the Atlantic Ocean, Biogeosciences, 7, 3167–3176, https://doi.org/10.5194/bg-7-3167-2010, 2010.

Fernandez, C., González, M. L., Muñoz, C., Molina, V., and Farias, L.: Temporal and spatial variability of biological nitrogen fixation off the upwelling system of central

Chile (35–38.5° S), J. Geophys. Res.-Oceans, 120, 3330–3349, https://doi.org/10.1002/2014jc010410, 2015.

Fernández-Castro, B., Mouriño-Carballido, B., Marañón, E., Chouciño, P., Gago, J., Ramírez, T., Vidal, M., Bode, A., Blasco, D., Royer, S.-J., Estrada, M., and Simó, R.: Importance of salt fingering for new nitrogen supply in the oligotrophic ocean, Nat. Commun., 6, 8002, https://doi.org/10.1038/ncomms9002, 2015.

Filella, A., Riemann, L., Van Wambeke, F., Pulido-Villena, E., Vogts, A., Bonnet, S., Grosso, O., Diaz, J. M., Duhamel, S., and Benavides, M.: Contrasting Roles of DOP as a Source of Phosphorus and Energy for Marine Diazotrophs, Front. Marine Sci., 9, 923765, https://doi.org/10.3389/fmars.2022.923765, 2022.

Flett, R. J., Hamilton, R. D., and Campbell, N. E. R.: Aquatic acetylene-reduction techniques: solutions to several problems, Can. J. Microbiol., 221, 43–51, https://doi.org/10.1139/m76-006, 1976.

Fonseca-Batista, D., Dehairs, F., Riou, V., Fripiat, F., Elskens, M., Deman, F., Brion, N., Quéroué, F., Bode, M., and Auel, H.: Nitrogen fixation in the eastern Atlantic reaches similar levels in the Southern and Northern Hemisphere, J. Geophys. Res.-Oceans, 122, 587–601, https://doi.org/10.1002/2016jc012335, 2017.

Fonseca-Batista, D., Li, X., Riou, V., Michotey, V., Deman, F., Fripiat, F., Guasco, S., Brion, N., Lemaitre, N., Tonnard, M., Gallinari, M., Planquette, H., Planchon, F., Sarthou, G., Elskens, M., LaRoche, J., Chou, L., and Dehairs, F.: Evidence of high N$_2$ fixation rates in the temperate northeast Atlantic, Biogeosciences, 16, 999–1017, https://doi.org/10.5194/bg-16-999-2019, 2019.

Foster, R. A., Subramaniam, A., Mahaffey, C., Carpenter, E. J., Capone, D. G., and Zehr, J. P.: Influence of the Amazon River plume on distributions of free-living and symbiotic cyanobacteria in the western tropical north Atlantic Ocean, Limnol. Oceanogr., 52, 517–532, https://doi.org/10.4319/lo.2007.52.2.0517, 2007.

Foster, R. A., Paytan, A., and Zehr, J.: Seasonality of N$_2$ fixation and *nifH* gene diversity in the Gulf of Aqaba (Red Sea), Limnol. Oceanogr., 54, 219–233, https://doi.org/10.4319/lo.2009.54.1.0219, 2009.

Foster, R. A., Kuypers, M. M. M., Vagner, T., Paerl, R. W., Musat, N., and Zehr, J. P.: Nitrogen fixation and transfer in open ocean diatom–cyanobacterial symbioses, ISME J., 5, 1484–1493, https://doi.org/10.1038/ismej.2011.26, 2011.

Foster, R. A., Sztejrenszus, S., and Kuypers, M. M. M.: Measuring carbon and N$_2$ fixation in field populations of colonial and free-living unicellular cyanobacteria using nanometer-scale secondary ion mass spectrometry, J. Phycol., 49, 502–516, https://doi.org/10.1111/jpy.12057, 2013.

Foster, R. A., Tienken, D., Littmann, S., Whitehouse, M. J., Kuypers, M. M. M., and White, A. E.: The rate and fate of N$_2$ and C fixation by marine diatom-diazotroph symbioses, ISME J., 16, 477–487, https://doi.org/10.1038/s41396-021-01086-7, 2022a.

Foster, R. A., Villareal, T. A., Lundin, D., Waterbury, J. B., Webb, E. A., and Zehr, J. P.: *Richelia*, in: Bergey's Manual of Systematics of Archaea and Bacteria, John Wiley & Sons, Inc., in association with Bergey's Manual Trust, 1–17, https://doi.org/10.1002/9781118960608.gbm01520, 2022b.

Gandhi, N., Singh, A., Prakash, S., Ramesh, R., Raman, M., Sheshshayee, M. S., and Shetye, S.: First direct measurements of N$_2$ fixation during a *Trichodesmium* bloom in the eastern Arabian Sea, Global Biogeochem. Cycles, 25, 1–10, https://doi.org/10.1029/2010gb003970, 2011.

Garcia, N., Raimbault, P., and Sandroni, V.: Seasonal nitrogen fixation and primary production in the Southwest Pacific: nanoplankton diazotrophy and transfer of nitrogen to picoplankton organisms, Marine Ecol. Prog. Ser., 343, 25–33, https://doi.org/10.3354/meps06882, 2007.

Geisler, E., Bogler, A., Bar-Zeev, E., and Rahav, E.: Heterotrophic nitrogen fixation at the hyper-eutrophic qshon river and estuary system, Front. Microbiol., 11, 1370, https://doi.org/10.3389/fmicb.2020.01370, 2020.

Giller, K. E., Nambiar, P. T. C., Srinivasa Rao, B., Dart, P. J., and Day, J. M.: A comparison of nitrogen fixation in genotypes of 420 groundnut (Arachis hypogaea L.) using ^{15}N-isotope dilution, Biol. Fert. Soils, 5, 23–25, https://doi.org/10.1007/BF00264341, 1987.

Glibert, P. M. and Bronk, D. A.: Release of Dissolved Organic Nitrogen by Marine Diazotrophic Cyanobacteria, *Trichodesmium* spp, Appl. Environ. Microbiol., 60, 3996–4000, https://doi.org/10.1128/aem.60.11.3996-4000.1994, 1994.

Glover, D. M., Jenkins, W. J., and Doney, S. C.: Modeling methods for marine science, Cambridge University Press, Cambridge, UK, https://doi.org/10.1017/CBO9780511975721, 2011.

Gradoville, M. R., Bombar, D., Crump, B. C., Letelier, R. M., Zehr, J. P., and White, A. E.: Diversity and activity of nitrogen-fixing communities across ocean basins, Limnol. Oceanogr., 62, 1895–1909, https://doi.org/10.1002/lno.10542, 2017.

Gradoville, M. R., Farnelid, H., White, A. E., Turk-Kubo, K. A., Stewart, B., Ribalet, F., Ferrón, S., Pinedo-Gonzalez, P., Armbrust, E. V., Karl, D. M., John, S., and Zehr, J. P.: Latitudinal constraints on the abundance and activity of the cyanobacterium UCYN-A and other marine diazotrophs in the North Pacific, Limnol. Oceanogr., 65, 1858–1875, https://doi.org/10.1002/lno.11423, 2020.

Gradoville, M., Cabello, A., Wilson, S., Turk-Kubo, K., Karl, D., and Zehr, J.: Light and depth dependency of nitrogen fixation by the non-photosynthetic, symbiotic cyanobacterium UCYN-A, Environ. Microbiol., 23, 4518–4531, https://doi.org/10.1111/1462-2920.15645, 2021.

Gradoville, M. R., Dugenne, M., Hynes, A. M., Zehr, J. P., and White, A. E.: Empirical relationship between *nifH* gene abundance and diazotroph cell concentration in the North Pacific Subtropical Gyre, J. Phycol., 53, 829–833, https://doi.org/10.1111/jpy.13289, 2022.

Graham, J. A., Argyle, M., and Furnham, A.: The goal structure of situations, Eur. J. Soc. Psychol., 10, 345–366, https://doi.org/10.1002/ejsp.2420100403, 1980.

Großkopf, T., Mohr, W., Baustian, T., Schunck, H., Gill, D., Kuypers, M. M. M., Lavik, G., Schmitz, R. A., Wallace, D. W. R., and LaRoche, J.: Doubling of marine dinitrogen-fixation rates based on direct measurements, Nature, 488, 361–364, https://doi.org/10.1038/nature11338, 2012.

Gruber, N.: The marine nitrogen cycle: overview and challenges, in: Nitrogen in the marine environment, 2nd edn., edited by: Capone, D. G., Bronk, D. A., Mulholland, M. R., and Carpenter, E. J., Elsevier, Amsterdam, 1–50, https://doi.org/10.1016/B978-0-12-372522-6.00001-3, 2008.

Gruber, N.: A diagnosis for marine nitrogen fixation, Nature, 566, 191–193, https://doi.org/10.1038/d41586-019-00498-y, 2019.

Hagino, K., Onuma, R., Kawachi, M., and Horiguchi, T.: Discovery of an Endosymbiotic Nitrogen-Fixing Cyanobacterium UCYN-A in Braarudosphaera bigelowii (Prymnesiophyceae), PLOS ONE, 8, e81749, https://doi.org/10.1371/journal.pone.0081749, 2013.

Hallstrøm, S., Benavides, M., Salamon, E. R., Arístegui, J., and Riemann, L.: Activity and distribution of diazotrophic communities across the Cape Verde Frontal Zone in the Northeast Atlantic Ocean, Biogeochemistry, 160, 49–67, https://doi.org/10.1007/s10533-022-00940-w, 2022.

Halm, H., Lam, P., Ferdelman, T. G., Lavik, G., Dittmar, T., LaRoche, J., D'Hondt, S., and Kuypers, M. M. M.: Heterotrophic organisms dominate nitrogen fixation in the South Pacific Gyre, ISME J., 6, 1238–1249, https://doi.org/10.1038/ismej.2011.182, 2012.

Hamersley, M. R., Turk, K. A., Leinweber, A., Gruber, N., Zehr, J. P., Gunderson, T., and Capone, D. G.: Nitrogen fixation within the water column associated with two hypoxic basins in the Southern California Bight, Aquat. Microb. Ecol., 63, 193–205, https://doi.org/10.3354/ame01494, 2011.

Harding, K., Turk-Kubo, K. A., Sipler, R. E., Mills, M. M., Bronk, D. A., and Zehr, J. P.: Symbiotic unicellular cyanobacteria fix nitrogen in the Arctic Ocean, P. Natl. Acad. Sci. USA, 115, 13371–13375, https://doi.org/10.1073/pnas.1813658115, 2018.

Harding, K. J., Turk-Kubo, K. A., Mak, E. W. K., Weber, P. K., Mayali, X., and Zehr, J. P.: Cell-specific measurements show nitrogen fixation by particle-attached putative non-cyanobacterial diazotrophs in the North Pacific Subtropical Gyre, Nat. Commun., 13, 6979, https://doi.org/10.1038/s41467-022-34585-y, 2022.

Hardy, R. W. F., Burns, R. C., and Holsten, R. D.: Applications of the acetylene-ethylene assay for measurement of nitrogen fixation, Soil Biol. Biochem., 5, 47–81, https://doi.org/10.1016/0038-0717(73)90093-X, 1973.

Harrison, P., Zingone, A., Mickelson, M., Lehtinen, S., Nagappa, R., Kraberg, A., Sun, J., McQuatters-Gollop, A., and Jakobsen, H.: Cell volumes of marine phytoplankton from globally distributed coastal data sets, Estuarine, Coast. Shelf Sci., 162, 130–142, https://doi.org/10.1016/j.ecss.2015.05.026, 2015.

Hashimoto, R., Watai, H., Miyahara, K., Sako, Y., and Yoshida, T.: Spatial and temporal variability of unicellular diazotrophic cyanobacteria in the eastern Seto Inland Sea, Fish. Sci., 82, 459–471, https://doi.org/10.1007/s12562-016-0983-y, 2016.

Hegde, S., Anil, A., Patil, J., Mitbavkar, S., Krishnamurthy, V., and Gopalakrishna, V.: Influence of environmental settings on the prevalence of Trichodesmium spp. in the Bay of Bengal, Mar. Ecol. Prog. Ser., 356, 93–101, https://doi.org/10.3354/meps07259, 2008.

Henke, B. A., Turk-Kubo, K. A., Bonnet, S., and Zehr, J. P.: Distributions and abundances of sublineages of the N₂-Fixing Cyanobacterium Candidatus Atelocyanobacterium thalassa (UCYN-A) in the New Caledonian Coral Lagoon, Front. Microbiol., 9, 554, https://doi.org/10.3389/fmicb.2018.00554, 2018.

Holl, C. M., Villareal, T. A., Payne, C. D., Clayton, T. D., Hart, C., and Montoya, J. P.: Trichodesmium in the western Gulf of Mexico: $^{15}N_2$-fixation and natural abundance stable isotopic evidence, Limnol. Oceanogr., 52, 2249–2259, https://doi.org/10.4319/lo.2007.52.5.2249, 2007.

Hörstmann, C., Raes, E. J., Buttigieg, P. L., Lo Monaco, C., John, U., and Waite, A. M.: Hydrographic fronts shape productivity, nitrogen fixation, and microbial community composition in the southern Indian Ocean and the Southern Ocean, Biogeosciences, 18, 3733–3749, https://doi.org/10.5194/bg-18-3733-2021, 2021.

Hyman, M. R. and Arp, D. J.: Quantification and removal of some contaminating gases from acetylene used to study gas-utilizing enzymes and microorganisms, Appl. Environ. Microbiol., 53, 298–303, https://doi.org/10.1128/aem.53.2.298-303.1987, 1987.

Ibello, V., Cantoni, C., Cozzi, S., and Civitarese, G.: First basin-wide experimental results on N₂ fixation in the open Mediterranean Sea, Geophys. Res. Lett., 37, L03608, https://doi.org/10.1029/2009gl041635, 2010.

Jayakumar, A., Chang, B. X., Widner, B., Bernhardt, P., Mulholland, M. R., and Ward, B. B.: Biological nitrogen fixation in the oxygen-minimum region of the eastern tropical North Pacific ocean, ISME J., 11, 2356–2367, https://doi.org/10.1038/ismej.2017.97, 2017.

Jiang, Z., Chen, J., Zhou, F., Zhai, H., Zhang, D., and Yan, X.: Summer distribution patterns of Trichodesmium spp. in the Changjiang (Yangtze River) Estuary and adjacent East China Sea shelf, Oceanologia, 59, 248–261, https://doi.org/10.1016/j.oceano.2017.02.001, 2017.

Jiang, Z., Zhu, Y., Sun, Z., Zhai, H., Zhou, F., Yan, X., Zeng, J., Chen, J., and Chen, Q.: Enhancement of Summer Nitrogen Fixation by the Kuroshio Intrusion in the East China Sea and Southern Yellow Sea, J. Geophys. Res.-Biogeo., 128, e2022JG007287, https://doi.org/10.1029/2022JG007287, 2023.

Karlusich, J. J. P., Pelletier, E., Lombard, F., Carsique, M., Dvorak, E., Colin, S., Picheral, M., Cornejo-Castillo, F. M., Acinas, S. G., Pepperkok, R., Karsenti, E., De Vargas, C., Wincker, P., Bowler, C., and Foster, R. A.: Global distribution patterns of marine nitrogen-fixers by imaging and molecular methods, Nat. Commun., 12, 4160, https://doi.org/10.1038/s41467-021-24299-y, 2021.

Kitajima, S., Furuya, K., Hashihama, F., Takeda, S., and Kanda, J.: Latitudinal distribution of diazotrophs and their nitrogen fixation in the tropical and subtropical western North Pacific, Limnol. Oceanogr., 54, 537–547, https://doi.org/10.4319/lo.2009.54.2.0537, 2009.

Kittu, L. R., Paul, A. J., Fernández-Méndez, M., Hopwood, M. J., and Riebesell, U.: Coastal N₂ Fixation Rates Coincide Spatially With Nitrogen Loss in the Humboldt Upwelling System off Peru, Global Biogeochem. Cycles, 37, e2022GB00757, https://doi.org/10.1029/2022gb007578, 2023.

Klawonn, I., Lavik, G., Boning, P., Marchant, H. K., Dekaezemacker, J., Mohr, W., and Ploug, H.: Simple approach for the preparation of $^{15-15}N_2$-enriched water for nitrogen fixation assessments: evaluation, application and recommendations, Front. Microbiol., 6, 769, https://doi.org/10.3389/fmicb.2015.00769, 2015.

Knapp, A. N., Casciotti, K. L., Berelson, W. M., Prokopenko, M. G., and Capone, D. G.: Low rates of nitrogen fixation in eastern tropical South Pacific surface waters, P. Natl. Acad. Sci. USA, 113, 4398–4403, https://doi.org/10.1073/pnas.1515641113, 2016.

Konno, U., Tsunogai, U., Komatsu, D. D., Daita, S., Nakagawa, F., Tsuda, A., Matsui, T., Eum, Y.-J., and Suzuki, K.: Determination of total N₂ fixation rates in the ocean taking into account both the

https://doi.org/10.5194/essd-15-3673-2023

Earth Syst. Sci. Data, 15, 3673–3709, 2023

particulate and filtrate fractions, Biogeosciences, 7, 2369–2377, https://doi.org/10.5194/bg-7-2369-2010, 2010.

Kromkamp, J., De Bie, M., Goosen, N., Peene, J., Van Rijswijk, P., Sinke, J., and Duinevel, G. C. A.: Primary production by phytoplankton along the Kenyan coast during the SE monsoon and November intermonsoon 1992, and the occurrence of *Trichodesmium*, Deep-Sea Res. Pt. II, 44, 1195–1212, https://doi.org/10.1016/s0967-0645(97)00015-5, 1997.

Krupke, A., Musat, N., LaRoche, J., Mohr, W., Fuchs, B. M., Amann, R. I., Kuypers, M. M. M., and Foster, R. A.: In situ identification and N₂ and C fixation rates of uncultivated cyanobacteria populations, Syst. Appl. Microbiol., 36, 259–271, https://doi.org/10.1016/j.syapm.2013.02.002, 2013.

Krupke, A., Lavik, G., Halm, H., Fuchs, B. M., Amann, R. I., and Kuypers, M. M. M.: Distribution of a consortium between unicellular algae and the N₂ fixing cyanobacterium UCYN-A in the North Atlantic Ocean, Environ. Microbiol., 16, 3153–3167, https://doi.org/10.1111/1462-2920.12431, 2014.

Krupke, A., Mohr, W., Laroche, J., Fuchs, B. M., Amann, R. I., and Kuypers, M. M.: The effect of nutrients on carbon and nitrogen fixation by the UCYN-A–haptophyte symbiosis, ISME J., 9, 1635–1647, https://doi.org/10.1038/ismej.2014.253, 2015.

Kumar, P. K., Singh, A., Ramesh, R., and Nallathambi, T.: N₂ Fixation in the eastern Arabian Sea: probable role of heterotrophic diazotrophs, Front. Marine Sci., 4, 80, https://doi.org/10.3389/fmars.2017.00080, 2017.

Kumari, V. R., Ghosh, V. R. D., Rao, D. N., Krishna, M. S., and Sarma, V. V. S. S.: Nitrogen fixation in the western coastal Bay of Bengal: Controlling factors and contribution to primary production, Regional Studies in Marine Science, 53, 102410, https://doi.org/10.1016/j.rsma.2022.102410, 2022.

Landou, E., Lazar, B., LaRoche, J., Fennel, K., and Berman-Frank, I.: Contribution of photic and aphotic N₂ fixation to production in an oligotrophic sea, Limnol. Oceanogr., 68, 692–708, https://doi.org/10.1002/lno.12303, 2023.

Langlois, R., Grokopf, T., Mills, M., Takeda, S., and LaRoche, J.: Widespread distribution and expression of Gamma A (UMB), an uncultured, diazotrophic, gamma-proteobacterial *nifH* phylotype, Plos One, 10, 17, https://doi.org/10.1371/journal.pone.0128912, 2015.

Le Moal, M. and Biegala, I. C.: Diazotrophic unicellular cyanobacteria in the northwestern Mediterranean Sea: A seasonal cycle, Limnol. Oceanogr., 54, 845–855, https://doi.org/10.4319/lo.2009.54.3.0845, 2009.

Le Moal, M., Collin, H., and Biegala, I. C.: Intriguing diversity among diazotrophic picoplankton along a Mediterranean transect: a dominance of rhizobia, Biogeosciences, 8, 827–840, https://doi.org/10.5194/bg-8-827-2011, 2011.

Letelier, R. and Karl, D.: Role of *Trichodesmium* spp. in the productivity of the subtropical North Pacific Ocean, Mar. Ecol. Prog. Ser., 133, 263–273, https://doi.org/10.3354/meps133263, 1996.

Li, L., Wu, C., Sun, J., Song, S., Ding, C., Huang, D., and Pujari, L.: Nitrogen fixation driven by mesoscale eddies and the Kuroshio Current in the northern South China Sea and the East China Sea, Acta Oceanol. Sin., 39, 30–41, https://doi.org/10.1007/s13131-020-1691-0, 2020.

Liu, J. X., Zhou, L. B., Li, J. J., Lin, Y. Y., Ke, Z. X., Zhao, C. Y., Liu, H. J., Jiang, X., He, Y. H., and Tan, Y. H.: Effect of mesoscale eddies on diazotroph com-munity structure and nitrogen fixation rates in the South China Sea, Regional Studies in Marine Science, 35, 14, https://doi.org/10.1016/j.rsma.2020.101106, 2020.

Loescher, C. R., Großkopf, T., Desai, F. D., Gill, D., Schunck, H., Croot, P. L., Schlosser, C., Neulinger, S. C., Pinnow, N., Lavik, G., Kuypers, M. M. M., LaRoche, J., and Schmitz, R. A.: Facets of diazotrophy in the oxygen minimum zone waters off Peru, ISME J., 8, 2180–2192, https://doi.org/10.1038/ismej.2014.71, 2014.

Loick-Wilde, N., Weber, S. C., Conroy, B. J., Capone, D. G., Coles, V. J., Medeiros, P. M., Steinberg, D. K., and Montoya, J. P.: Nitrogen sources and net growth efficiency of zooplankton in three Amazon River plume food webs, Limnol. Oceanogr., 61, 460–481, https://doi.org/10.1002/lno.10227, 2015.

Loick-Wilde, N., Fernandez-Urruzola, I., Eglite, E., Liskow, I., Nausch, M., Schulz-Bull, D., Wodarg, D., Wasmund, N., and Mohrholz, V.: Stratification, nitrogen fixation, and cyanobacterial bloom stage regulate the planktonic food web structure, Glob. Chang. Biol., 25, 794–810, https://doi.org/10.1111/gcb.14546, 2019.

Lory, C., Van Wambeke, F., Fourquez, M., Barani, A., Guieu, C., Tilliette, C., Marie, D., Nunige, S., Berman-Frank, I., and Bonnet, S.: Assessing the contribution of diazotrophs to microbial Fe uptake using a group specific approach in the Western Tropical South Pacific Ocean, ISME Commun., 2, 41, https://doi.org/10.1038/s43705-022-00122-7, 2022.

Löscher, C. R., Bourbonnais, A., Dekaezemacker, J., Charoenpong, C. N., Altabet, M. A., Bange, H. W., Czeschel, R., Hoffmann, C., and Schmitz, R.: N₂ fixation in eddies of the eastern tropical South Pacific Ocean, Biogeosciences, 13, 2889–2899, https://doi.org/10.5194/bg-13-2889-2016, 2016.

Löscher, C. R., Mohr, W., Bange, H. W., and Canfield, D. E.: No nitrogen fixation in the Bay of Bengal?, Biogeosciences, 17, 851–864, https://doi.org/10.5194/bg-17-851-2020, 2020.

Lu, Y., Wen, Z., Shi, D., Chen, M., Zhang, Y., Bonnet, S., Li, Y., Tian, J., and Kao, S.-J.: Effect of light on N₂ fixation and net nitrogen release of *Trichodesmium* in a field study, Biogeosciences, 15, 1–12, https://doi.org/10.5194/bg-15-1-2018, 2018.

Luo, Y.-W., Doney, S. C., Anderson, L. A., Benavides, M., Berman-Frank, I., Bode, A., Bonnet, S., Boström, K. H., Böttjer, D., Capone, D. G., Carpenter, E. J., Chen, Y. L., Church, M. J., Dore, J. E., Falcón, L. I., Fernández, A., Foster, R. A., Furuya, K., Gómez, F., Gundersen, K., Hynes, A. M., Karl, D. M., Kitajima, S., Langlois, R. J., LaRoche, J., Letelier, R. M., Marañón, E., McGillicuddy Jr., D. J., Moisander, P. H., Moore, C. M., Mouriño-Carballido, B., Mulholland, M. R., Needoba, J. A., Orcutt, K. M., Poulton, A. J., Rahav, E., Raimbault, P., Rees, A. P., Riemann, L., Shiozaki, T., Subramaniam, A., Tyrrell, T., Turk-Kubo, K. A., Varela, M., Villareal, T. A., Webb, E. A., White, A. E., Wu, J., and Zehr, J. P.: Database of diazotrophs in global ocean: abundance, biomass and nitrogen fixation rates, Earth Syst. Sci. Data, 4, 47–73, https://doi.org/10.5194/essd-4-47-2012, 2012.

Luo, Y.-W., Lima, I. D., Karl, D. M., Deutsch, C. A., and Doney, S. C.: Data-based assessment of environmental controls on global marine nitrogen fixation, Biogeosciences, 11, 691–708, https://doi.org/10.5194/bg-11-691-2014, 2014.

Mague, T. H., Weare, N. M., and Holm-Hansen, O.: Nitrogen fixation in the North Pacific Ocean, Mar. Biol., 24, 109–119, https://doi.org/10.1007/bf00389344, 1974.

Martínez-Pérez, C., Mohr, W., Loscher, C. R., Dekaezemacker, J., Littmann, S., Yilmaz, P., Lehnen, N., Fuchs, B. M., Lavik, G., Schmitz, R. A., LaRoche, J., and Kuypers, M. M.: The small unicellular diazotrophic symbiont, UCYN-A, is a key player in the marine nitrogen cycle, Nat. Microbiol., 1, 16163, https://doi.org/10.1038/nmicrobiol.2016.163, 2016.

Masotti, I., Ruiz-Pino, D., and Le Bouteiller, A.: Photosynthetic characteristics of *Trichodesmium* in the southwest Pacific Ocean: importance and significance, Mar. Ecol. Prog. Ser., 338, 47–59, https://doi.org/10.3354/meps338047, 2007.

McCarthy, J. J. and Carpenter, E. J.: Oscillatoria (*Trichodesmium*) Thiebautii (cyanophyta) the central North Atlantic Ocean, J. Phycol., 15, 75–82, https://doi.org/10.1111/j.1529-8817.1979.tb02965.x, 1979.

Meiler, S., Britten, G. L., Dutkiewicz, S., Gradoville, M. R., Moisander, P. H., Jahn, O., and Follows, M. J.: Constraining uncertainties of diazotroph biogeography from *nifH* gene abundance, Limnol. Oceanogr., 67, 816–829, https://doi.org/10.1002/lno.12036, 2022.

Meiler, S., Britten, G. L., Dutkiewicz, S., Moisander, P. H., and Follows, M. J.: Challenges and opportunities in connecting gene count observations with ocean biogeochemical models: Reply to Zehr and Riemann (2023), Limnol. Oceanogr., 68, 1413–1416, https://doi.org/10.1002/lno.12363, 2023.

Menden-Deuer, S. and Lessard, E. J.: Carbon to volume relationships for dinoflagellates, diatoms, and other protist plankton, Limnol. Oceanogr., 45, 569–579, https://doi.org/10.4319/lo.2000.45.3.0569, 2000.

Messer, L. F., Mahaffey, C., M Robinson, C., Jeffries, T. C., Baker, K. G., Bibiloni Isaksson, J., Ostrowski, M., Doblin, M. A., Brown, M. V., and Seymour, J. R.: High levels of heterogeneity in diazotroph diversity and activity within a putative hotspot for marine nitrogen fixation, ISME J., 10, 1499–1513, https://doi.org/10.1038/ismej.2015.205, 2016.

Messer, L. F., Brown, M. V., Van Ruth, P. D., Doubell, M., and Seymour, J. R.: Temperate southern Australian coastal waters are characterised by surprisingly high rates of nitrogen fixation and diversity of diazotrophs, PeerJ, 9, e10809, https://doi.org/10.7717/peerj.10809, 2021.

Meyer, N. R., Fortney, J. L., and Dekas, A. E.: NanoSIMS sample preparation decreases isotope enrichment: magnitude, variability and implications for single-cell rates of microbial activity, Environ. Microbiol., 23, 81–98, https://doi.org/10.1111/1462-2920.15264, 2021.

Mills, M. M., Turk-Kubo, K. A., van Dijken, G. L., Henke, B. A., Harding, K., Wilson, S. T., Arrigo, K. R., and Zehr, J. P.: Unusual marine cyanobacteria/haptophyte symbiosis relies on N₂ fixation even in N-rich environments, ISME J., 14, 2395–2406, https://doi.org/10.1038/s41396-020-0691-6, 2020.

Mohr, W., Grosskopf, T., Wallace, D. W., and LaRoche, J.: Methodological underestimation of oceanic nitrogen fixation rates, PLoS One, 5, e12583, https://doi.org/10.1371/journal.pone.0012583, 2010.

Moisander, P. H., Zhang, R., Boyle, E. A., Hewson, I., Montoya, J. P., and Zehr, J. P.: Analogous nutrient limitations in unicellular diazotrophs and *Prochlorococcus* in the South Pacific Ocean, ISME J., 6, 733–744, https://doi.org/10.1038/ismej.2011.152, 2012.

Moisander, P. H., Serros, T., Paerl, R. W., Beinart, R. A., and Zehr, J. P.: Gammaproteobacterial diazotrophs and *nifH* gene expression in surface waters of the South Pacific Ocean, ISME J, 8, 1962–1973, https://doi.org/10.1038/ismej.2014.49, 2014.

Moisander, P. H., Benavides, M., Bonnet, S., Berman-Frank, I., White, A. E., and Riemann, L.: Chasing after non-cyanobacterial nitrogen fixation in marine pelagic environments, Front. Microbiol., 8, 1736, https://doi.org/10.3389/fmicb.2017.01736, 2017.

Mompeán, C., Bode, A., Benítez-Barrios, V. M., Domínguez-Yanes, J. F., Escánez, J., and Fraile-Nuez, E.: Spatial patterns of plankton biomass and stable isotopes reflect the influence of the nitrogen-fixer Trichodesmium along the subtropical North Atlantic, J. Plankton Res., 35, 513–525, https://doi.org/10.1093/plankt/fbt011, 2013.

Mompeán, C., Bode, A., Latasa, M., Fernández-Castro, B., Mouriño-Carballido, B., and Irigoien, X.: The influence of nitrogen inputs on biomass and trophic structure of ocean plankton: a study using biomass and stable isotope size-spectra, J. Plankton Res., 38, 1163–1177, https://doi.org/10.1093/plankt/fbw052, 2016.

Montoya, J. P., Voss, M., Kahler, P., and Capone, D. G.: A Simple, High-Precision, High-Sensitivity Tracer Assay for N₂ Fixation, Appl. Environ. Microbiol., 62, 986–993, https://doi.org/10.1128/aem.62.3.986-993.1996, 1996.

Moore, R. M., Grefe, I., Zorz, J., Shan, S., Thompson, K., Ratten, J., and LaRoche, J.: On the relationship between hydrogen saturation in the tropical Atlantic Ocean and nitrogen fixation by the symbiotic diazotroph UCYN-A, J. Geophys. Res.-Oceans, 123, 2353–2362, https://doi.org/10.1002/2017jc013047, 2018.

Moreira-Coello, V., Mourino-Carballido, B., Maranon, E., Fernandez-Carrera, A., Bode, A., and Varela, M. M.: Biological N₂ fixation in the upwelling region off NW Iberia: magnitude, relevance, and players, Front. Mar. Sci., 4, 303, https://doi.org/10.3389/fmars.2017.00303, 2017.

Mulholland, M. R.: The fate of nitrogen fixed by diazotrophs in the ocean, Biogeosciences, 4, 37–51, https://doi.org/10.5194/bg-4-37-2007, 2007.

Mulholland, M. R., Bernhardt, P. W., Heil, C. A., Bronk, D. A., and O'Neil, J. M.: Nitrogen fixation and release of fixed nitrogen by *Trichodesmium* spp. in the Gulf of Mexico, Limnol. Oceanogr., 51, 1762–1776, https://doi.org/10.4319/lo.2006.51.4.1762, 2006.

Mulholland, M. R., Bernhardt, P. W., Blanco-Garcia, J. L., Mannino, A., Hyde, K., Mondragon, E., Turk, K., Moisander, P. H., and Zehr, J. P.: Rates of dinitrogen fixation and the abundance of diazotrophs in North American coastal waters between Cape Hatteras and Georges Bank, Limnol. Oceanogr., 57, 1067–1083, https://doi.org/10.4319/lo.2012.57.4.1067, 2012.

Mulholland, M. R., Bernhardt, P. W., Widner, B. N., Selden, C. R., Chappell, P. D., Clayton, S., Mannino, A., and Hyde, K.: High rates of N₂ fixation in temperate, western North Atlantic coastal waters expand the realm of marine diazotrophy, Global Biogeochem. Cycles, 33, 826–840, https://doi.org/10.1029/2018gb006130, 2019.

Musat, N., Stryhanyuk, H., Bombach, P., Adrian, L., Audinot, J.-N., and Richnow, H. H.: The effect of FISH and CARD-FISH on the isotopic composition of 13C- and 15N-labeled Pseudomonas

https://doi.org/10.5194/essd-15-3673-2023

Earth Syst. Sci. Data, 15, 3673–3709, 2023

putida cells measured by nanoSIMS, Syst. Appl. Microbiol., 37, 267–276, https://doi.org/10.1016/j.syapm.2014.02.002, 2014.

Needoba, J. A., Foster, R. A., Sakamoto, C., Zehr, J. P., and Johnson, K. S.: Nitrogen fixation by unicellular diazotrophic cyanobacteria in the temperate oligotrophic North Pacific Ocean, Limnol. Oceanogr., 52, 1317–1327, https://doi.org/10.4319/lo.2007.52.4.1317, 2007.

Palter, J. B., Ames, E. J., Benavides, M., Goncalves Neto, A., Granger, J., Moisander, P. H., Watkins-Brandt, K. S., and White, A. E.: High N₂ fixation in and near the Gulf Stream consistent with a circulation control on diazotrophy, Geophys. Res. Lett., 47, e2020GL089103, https://doi.org/10.1111/j.1365-2656.2010.01695.x, 2020.

Postgate, J. R.: Nitrogen Fixation, 3rd Edn., Cambridge University Press, Cambridge, United Kingdom, 1998.

Raes, E., van de Kamp, J., Bodrossy, L., Fong, A., Riekenberg, J., Holmes, B., Erler, D., Eyre, B., Weil, S.-S., and Waite, A.: N₂ fixation and new insights into nitrification from the ice-edge to the equator in the South Pacific Ocean, Front. Marine Sci., 7, 389, https://doi.org/10.3389/fmars.2020.00389, 2020.

Raes, E. J., Waite, A. M., McInnes, A. S., Olsen, H., Nguyen, H. M., Hardman-Mountford, N., and Thompson, P. A.: Changes in latitude and dominant diazotrophic community alter N₂ fixation, Marine Ecol. Prog. Ser., 516, 85–102, https://doi.org/10.3354/meps11009, 2014.

Rahav, E., Bar-Zeev, E., Ohayon, S., Elifantz, H., Belkin, N., Herut, B., Mulholland, M. R., and Berman-Frank, I.: Dinitrogen fixation in aphotic oxygenated marine environments, Front. Microbiol., 4, 227, https://doi.org/10.3389/fmicb.2013.00227, 2013a.

Rahav, E., Herut, B., Levi, A., Mulholland, M. R., and Berman-Frank, I.: Springtime contribution of dinitrogen fixation to primary production across the Mediterranean Sea, Ocean Sci., 9, 489–498, https://doi.org/10.5194/os-9-489-2013, 2013b.

Rahav, E., Herut, B., Mulholland, M., Belkin, N., Elifantz, H., and Berman-Frank, I.: Heterotrophic and autotrophic contribution to dinitrogen fixation in the Gulf of Aqaba, Marine Ecol. Prog. Ser., 522, 67–77, https://doi.org/10.3354/meps11143, 2015.

Rahav, E., Giannetto, M. J., and Bar-Zeev, E.: Contribution of mono and polysaccharides to heterotrophic N₂ fixation at the eastern Mediterranean coastline, Sci. Rep.-UK, 6, 27858, https://doi.org/10.1038/srep27858, 2016.

Ratten, J.-M., LaRoche, J., Desai, D. K., Shelley, R. U., Landing, W. M., Boyle, E., Cutter, G. A., and Langlois, R. J.: Sources of iron and phosphate affect the distribution of diazotrophs in the North Atlantic, Deep-Sea Res. Pt. II, 116, 332–341, https://doi.org/10.1016/j.dsr2.2014.11.012, 2015.

Reeder, C. F., Stoltenberg, I., Javidpour, J., and Löscher, C. R.: Salinity as a key control on the diazotrophic community composition in the southern Baltic Sea, Ocean Sci., 18, 401–417, https://doi.org/10.5194/os-18-401-2022, 2022.

Riou, V., Fonseca-Batista, D., Roukaerts, A., Biegala, I. C., Prakya, S. R., Magalhães Loureiro, C., Santos, M., Muniz-Piniella, A. E., Schmiing, M., Elskens, M., Brion, N., Martins, M. A., and Dehairs, F.: Importance of N₂-fixation on the productivity at the North-Western Azores Current/Front System, and the abundance of diazotrophic unicellular cyanobacteria, PLoS One, 11, e0150827, https://doi.org/10.1371/journal.pone.0150827, 2016.

Sahoo, D., Saxena, H., Nazirahmed, S., Kumar, S., Sudheer, A. K., Bhushan, R., Sahay, A., and Singh, A.: Role of eddies and N₂ fixation in regulating C : N : P proportions in the Bay of Bengal, Biogeochemistry, 155, 413–429, https://doi.org/10.1007/s10533-021-00833-4, 2021.

Sahu, B. K., Baliarsingh, S. K., Lotliker, A. A., Parida, C., Srichandan, S., and Sahu, K. C.: Winter thermal inversion and *Trichodesmium* dominance in north-western Bay of Bengal, Ocean Sci. J., 52, 301–306, https://doi.org/10.1007/s12601-017-0028-1, 2017.

Sargent, E. C., Hitchcock, A., Johansson, S. A., Langlois, R., Moore, C. M., LaRoche, J., Poulton, A. J., and Bibby, T. S.: Evidence for polyploidy in the globally important diazotroph *Trichodesmium*, FEMS Microbiol. Lett., 363, fnw244, https://doi.org/10.1093/femsle/fnw244, 2016.

Sarma, V. V. S. S., Vivek, R., Rao, D. N., and Ghosh, V. R. D.: Severe phosphate limitation on nitrogen fixation in the Bay of Bengal, Cont. Shelf Res., 205, 104199, https://doi.org/10.1016/j.csr.2020.104199, 2020.

Sato, T., Shiozaki, T., Taniuchi, Y., Kasai, H., and Takahashi, K.: Nitrogen fixation and diazotroph community in the subarctic Sea of Japan and Sea of Okhotsk, J. Geophys. Res.-Oceans, 126, e2020JC017071, https://doi.org/10.1029/2020jc017071, 2021.

Sato, T., Shiozaki, T., Hashihama, F., Sato, M., Murata, A., Sasaoka, K., Umeda, S.-i., and Takahashi, K.: Low Nitrogen Fixation Related to Shallow Nitracline Across the Eastern Indian Ocean, J. Geophys. Res.-Biogeo., 127, e2022JG007104, https://doi.org/10.1029/2022JG007104, 2022.

Saulia, E., Benavides, M., Henke, B., Turk-Kubo, K., Cooperguard, H., Grosso, O., Desnues, A., Rodier, M., Dupouy, C., Riemann, L., and Bonnet, S.: Seasonal Shifts in Diazotrophs Players: Patterns Observed Over a Two-Year Time Series in the New Caledonian Lagoon (Western Tropical South Pacific Ocean), Front. Marine Sci., 7, 581755, https://doi.org/10.3389/fmars.2020.581755, 2020.

Saxena, H., Sahoo, D., Khan, M. A., Kumar, S., Sudheer, A. K., and Singh, A.: Dinitrogen fixation rates in the Bay of Bengal during summer monsoon, Environ. Res. Commun., 2, 051007, https://doi.org/10.1088/2515-7620/ab89fa, 2020.

Scavotto, R. E., Dziallas, C., Bentzon-Tilia, M., Riemann, L., and Moisander, P. H.: Nitrogen-fixing bacteria associated with copepods in coastal waters of the North Atlantic Ocean, Environ. Microbiol., 17, 3754–3765, https://doi.org/10.1111/1462-2920.12777, 2015.

Schvarcz, C. R., Wilson, S. T., Caffin, M., Stancheva, R., Li, Q., Turk-Kubo, K. A., White, A. E., Karl, D. M., Zehr, J. P., and Steward, G. F.: Overlooked and widespread pennate diatom-diazotroph symbioses in the sea, Nat. Commun., 13, 799, https://doi.org/10.1038/s41467-022-28065-6, 2022.

Selden, C. R., Mulholland, M. R., Bernhardt, P. W., Widner, B., Macías-Tapia, A., Ji, Q., and Jayakumar, A.: Dinitrogen Fixation Across Physico-Chemical Gradients of the Eastern Tropical North Pacific Oxygen Deficient Zone, Global Biogeochem. Cycles, 33, 1187–1202, https://doi.org/10.1029/2019gb006242, 2019.

Selden, C. R., Chappell, P. D., Clayton, S., Macías-Tapia, A., Bernhardt, P. W., and Mulholland, M. R.: A coastal N₂ fixation hotspot at the Cape Hatteras front: Elucidating spatial heterogeneity in diazotroph activity via supervised machine learning, Limnol. Oceanogr., 66, 1832–1849, https://doi.org/10.1002/lno.11727, 2021a.

Selden, C. R., Mulholland, M. R., Widner, B., Bernhardt, P., and Jayakumar, A.: Toward resolving disparate accounts of the extent and magnitude of nitrogen fixation in the Eastern Tropical South Pacific oxygen deficient zone, Limnol. Oceanogr., 66, 1950–1960, https://doi.org/10.1002/lno.11735, 2021b.

Selden, C. R., Einarsson, S. V., Lowry, K. E., Crider, K. E., Pickart, R. S., Lin, P., Ashjian, C. J., and Chappell, P. D.: Coastal upwelling enhances abundance of a symbiotic diazotroph (UCYN-A) and its haptophyte host in the Arctic Ocean, Front. Mar. Sci., 9, 877562, https://doi.org/10.3389/fmars.2022.877562, 2022.

Shao, Z. and Luo, Y.-W.: Controlling factors on the global distribution of a representative marine non-cyanobacterial diazotroph phylotype (Gamma A), Biogeosciences, 19, 2939–2952, https://doi.org/10.5194/bg-19-2939-2022, 2022.

Shao, Z., Xu, Y., Wang, H., Luo, W., Wang, L., Huang, Y., and Luo, Y.-W.: Version 2 of the global oceanic diazotroph database, Figshare [data set], https://doi.org/10.6084/m9.figshare.21677687, 2022.

Shiozaki, T., Kodama, T., Kitajima, S., Sato, M., and Furuya, K.: Advective transport of diazotrophs and importance of their nitrogen fixation on new and primary production in the western Pacific warm pool, Limnol. Oceanogr., 58, 49–60, https://doi.org/10.4319/lo.2013.58.1.0049, 2013.

Shiozaki, T., Chen, Y. L. L., Lin, Y. H., Taniuchi, Y., Sheu, D. S., Furuya, K., and Chen, H. Y.: Seasonal variations of unicellular diazotroph groups A and B, and *Trichodesmium* in the northern South China Sea and neighboring upstream Kuroshio Current, Cont. Shelf Res., 80, 20–31, https://doi.org/10.1016/j.csr.2014.02.015, 2014a.

Shiozaki, T., Ijichi, M., Kodama, T., Takeda, S., and Furuya, K.: Heterotrophic bacteria as major nitrogen fixers in the euphotic zone of the Indian Ocean, Global Biogeochem. Cycles, 28, 1096–1110, https://doi.org/10.1002/2014gb004886, 2014b.

Shiozaki, T., Kodama, T., and Furuya, K.: Large-scale impact of the island mass effect through nitrogen fixation in the western South Pacific Ocean, Geophys. Res. Lett., 41, 2907–2913, https://doi.org/10.1002/2014GL059835, 2014c.

Shiozaki, T., Nagata, T., Ijichi, M., and Furuya, K.: Nitrogen fixation and the diazotroph community in the temperate coastal region of the northwestern North Pacific, Biogeosciences, 12, 4751–4764, https://doi.org/10.5194/bg-12-4751-2015, 2015a.

Shiozaki, T., Takeda, S., Itoh, S., Kodama, T., Liu, X., Hashihama, F., and Furuya, K.: Why is *Trichodesmium* abundant in the Kuroshio?, Biogeosciences, 12, 6931–6943, https://doi.org/10.5194/bg-12-6931-2015, 2015b.

Shiozaki, T., Bombar, D., Riemann, L., Hashihama, F., Takeda, S., Yamaguchi, T., Ehama, M., Hamasaki, K., and Furuya, K.: Basin scale variability of active diazotrophs and nitrogen fixation in the North Pacific, from the tropics to the subarctic Bering Sea, Global Biogeochem. Cycles, 31, 996–1009, https://doi.org/10.1002/2017gb005681, 2017.

Shiozaki, T., Bombar, D., Riemann, L., Sato, M., Hashihama, F., Kodama, T., Tanita, I., Takeda, S., Saito, H., Hamasaki, K., and Furuya, K.: Linkage Between Dinitrogen Fixation and Primary Production in the Oligotrophic South Pacific Ocean, Global Biogeochem. Cycles, 32, 1028–1044, https://doi.org/10.1029/2017GB005869, 2018a.

Shiozaki, T., Fujiwara, A., Ijichi, M., Harada, N., Nishino, S., Nishi, S., Nagata, T., and Hamasaki, K.: Diazotroph community structure and the role of nitrogen fixation in the nitrogen cycle in the Chukchi Sea (western Arctic Ocean), Limnol. Oceanogr., 63, 2191–2205, https://doi.org/10.1002/lno.10933, 2018b.

Shiozaki, T., Kondo, Y., Yuasa, D., and Takeda, S.: Distribution of major diazotrophs in the surface water of the Kuroshio from northeastern Taiwan to south of mainland Japan, J. Plankton Res., 40, 407–419, https://doi.org/10.1093/plankt/fby027, 2018c.

Shiozaki, T., Fujiwara, A., Inomura, K., Hirose, Y., Hashihama, F., and Harada, N.: Biological nitrogen fixation detected under Antarctic sea ice, Nat. Geosci., 13, 729, https://doi.org/10.1038/s41561-020-00651-7, 2020.

Short, S. M. and Zehr, J. P.: Quantitative Analysis of *nifH* Genes and Transcripts from Aquatic Environments, in: Methods in Enzymology, Academic Press, 397, 380–394, https://doi.org/10.1016/S0076-6879(05)97023-7, 2005.

Singh, A., Bach, L. T., Fischer, T., Hauss, H., Kiko, R., Paul, A. J., Stange, P., Vandromme, P., and Riebesell, U.: Niche construction by non-diazotrophs for N₂ fixers in the eastern tropical North Atlantic Ocean, Geophys. Res. Lett., 44, 6904–6913, https://doi.org/10.1002/2017gl074218, 2017.

Singh, A., Gandhi, N., and Ramesh, R.: Surplus supply of bioavailable nitrogen through N₂ fixation to primary producers in the eastern Arabian Sea during autumn, Cont. Shelf Res., 181, 103–110, https://doi.org/10.1016/j.csr.2019.05.012, 2019.

Sipler, R. E., Gong, D., Baer, S. E., Sanderson, M. P., Roberts, Q. N., Mulholland, M. R., and Bronk, D. A.: Preliminary estimates of the contribution of Arctic nitrogen fixation to the global nitrogen budget, Limnol. Oceanogr. Lett., 2, 159–166, https://doi.org/10.1002/lol2.10046, 2017.

Sohm, J. A., Hilton, J. A., Noble, A. E., Zehr, J. P., Saito, M. A., and Webb, E. A.: Nitrogen fixation in the South Atlantic Gyre and the Benguela upwelling system, Geophys. Res. Lett., 38, L16608, https://doi.org/10.1029/2011GL048315, 2011.

Staal, M., Lintel-Hekkert, S. t., Harren, F., and Stal, L.: Nitrogenase activity in cyanobacteria measured by the acetylene reduction assay: a comparison between batch incubation and on-line monitoring, Environ. Microbiol., 3, 343–351, https://doi.org/10.1046/j.1462-2920.2001.00201.x, 2001.

Staal, M., te Lintel Hekkert, S., Jan Brummer, G., Veldhuis, M., Sikkens, C., Persijn, S., and Stal, L. J.: Nitrogen fixation along a north-south transect in the eastern Atlantic Ocean, Limnol. Oceanogr., 52, 1305–1316, https://doi.org/10.4319/lo.2007.52.4.1305, 2007.

Stenegren, M., Berg, C., Padilla, C., David, S.-S., Montoya, J., Yager, P., and Foster, R.: Piecewise Structural Equation Model (SEM) Disentangles the Environmental Conditions Favoring Diatom Diazotroph Associations (DDAs) in the Western Tropical North Atlantic (WTNA), Front. Microbiol., 8, 810, https://doi.org/10.3389/fmicb.2017.00810, 2017.

Stenegren, M., Caputo, A., Berg, C., Bonnet, S., and Foster, R. A.: Distribution and drivers of symbiotic and free-living diazotrophic cyanobacteria in the western tropical South Pacific, Biogeosciences, 15, 1559–1578, https://doi.org/10.5194/bg-15-1559-2018, 2018.

Subramaniam, A., Yager, P., Carpenter, E., Mahaffey, C., Björkman, K., Cooley, S., Kustka, A., Montoya, J., Sañudo-Wilhelmy, S., and Shipe, R.: Amazon River enhances diazotrophy and carbon sequestration in the tropical North At-

lantic Ocean, P. Natl. Acad. Sci. USA, 105, 10460–10465, https://doi.org/10.1073/pnas.0710279105, 2008.

Subramaniam, A., Mahaffey, C., Johns, W., and Mahowald, N.: Equatorial upwelling enhances nitrogen fixation in the Atlantic Ocean, Geophys. Res. Lett., 40, 1766–1771, https://doi.org/10.1002/grl.50250, 2013.

Suzuki, S., Kawachi, M., Tsukakoshi, C., Nakamura, A., Hagino, K., Inouye, I., and Ishida, K.-I.: Unstable relationship between *Braarudosphaera bigelowii* (= *Chrysochromulina parkeae*) and its nitrogen-fixing endosymbiont, Front. Plant Sci., 12, 749895, https://doi.org/10.3389/fpls.2021.749895, 2021.

Tang, W., Cerdán-García, E., Berthelot, H., Polyviou, D., Wang, S., Baylay, A., Whitby, H., Planquette, H., Mowlem, M., Robidart, J., and Cassar, N.: New insights into the distributions of nitrogen fixation and diazotrophs revealed by high-resolution sensing and sampling methods, ISME J., 14, 2514–2526, https://doi.org/10.1038/s41396-020-0703-6, 2020.

Tang, W. Y. and Cassar, N.: Data-driven modeling of the distribution of diazotrophs in the global ocean, Geophys. Res. Lett., 46, 12258–12269, https://doi.org/10.1029/2019gl084376, 2019.

Tang, W. Y., Wang, S., Fonseca-Batista, D., Dehairs, F., Gifford, S., Gonzalez, A. G., Gallinari, M., Planquette, H., Sarthou, G., and Cassar, N.: Revisiting the distribution of oceanic N₂ fixation and estimating diazotrophic contribution to marine production, Nat. Commun., 10, https://doi.org/10.1038/s41467-019-08640-0, 2019.

Tenório, M. M. B., Dupouy, C., Rodier, M., and Neveux, J.: *Trichodesmium* and other planktonic cyanobacteria in New Caledonian waters (SW tropical Pacific) during an El Niño episode, Aquat. Microb. Ecol., 81, 219–241, https://doi.org/10.3354/ame01873, 2018.

Thomas, B. L. K.: Geometric means and measures of dispersion, Biometrics, 35, 908–909, 1979.

Thompson, A., Carter, B. J., Turk-Kubo, K., Malfatti, F., Azam, F., and Zehr, J. P.: Genetic diversity of the unicellular nitrogen-fixing cyanobacteria UCYN-A and its prymnesiophyte host, Environ. Microbiol., 16, 3238–3249, https://doi.org/10.1111/1462-2920.12490, 2014.

Thompson, A. W., Foster, R. A., Krupke, A., Carter, B. J., Musat, N., Vaulot, D., Kuypers, M. M. M., and Zehr, J. P.: Unicellular cyanobacterium symbiotic with a single-celled eukaryotic alga, Science, 337, 1546–1550, https://doi.org/10.1126/science.1222700, 2012.

Tuo, S.-h., Mulholland, M. R., Taniuchi, Y., Chen, H.-Y., Jane, W.-N., Lin, Y.-H., and Chen, Y.-l. L.: Trichome lengths of the heterocystous N₂-fixing cyanobacteria in the tropical marginal seas of the western north pacific, Front. Marine Sci., 8, 678607, https://doi.org/10.3389/fmars.2021.678607, 2021.

Turk-Kubo, K., Achilles, K., Serros, T., Ochiai, M., Montoya, J., and Zehr, J.: Nitrogenase (*nifH*) gene expression in diazotrophic cyanobacteria in the Tropical North Atlantic in response to nutrient amendments., Front. Aquat. Microbiol., 3, 1–17, https://doi.org/10.3389/fmicb.2012.00386, 2012.

Turk-Kubo, K. A., Karamchandani, M., Capone, D. G., and Zehr, J. P.: The paradox of marine heterotrophic nitrogen fixation: abundances of heterotrophic diazotrophs do not account for nitrogen fixation rates in the Eastern Tropical South Pacific, Environ. Microbiol., 16, 3095–3114, https://doi.org/10.1111/1462-2920.12346, 2014.

Turk-Kubo, K. A., Mills, M. M., Arrigo, K. R., van Dijken, G., Henke, B. A., Stewart, B., Wilson, S. T., and Zehr, J. P.: UCYN-A/haptophyte symbioses dominate N₂ fixation in the Southern California Current System, ISME Commun., 1, 42, https://doi.org/10.1038/s43705-021-00039-7, 2021.

Turk-Kubo, K., Gradoville, M., Cheung, S., Cornejo Castillo, F. M., Harding, K., Morando, M., Mills, M., and Zehr, J.: Non-cyanobacterial diazotrophs: Global diversity, distribution, ecophysiology, and activity in marine waters, FEMS Microbiol. Rev., fuac046, https://doi.org/10.1093/femsre/fuac046, 2022.

Verity, P. G., Robertson, C. Y., Tronzo, C. R., Andrews, M. G., Nelson, J. R., and Sieracki, M. E.: Relationships between cell volume and the carbon and nitrogen content of marine photosynthetic nanoplankton, Limnol. Oceanogr., 37, 1434–1446, https://doi.org/10.4319/lo.1992.37.7.1434, 1992.

Villareal, T. A., Adornato, L., Wilson, C., and Schoenbaechler, C. A.: Summer blooms of diatom-diazotroph assemblages and surface chlorophyll in the North Pacific gyre: A disconnect, J. Geophys. Res., 116, C03001, https://doi.org/10.1029/2010jc006268, 2011.

Wang, S., Tang, W., Delage, E., Gifford, S., Whitby, H., González, A. G., Eveillard, D., Planquette, H., and Cassar, N.: Investigating the microbial ecology of coastal hotspots of marine nitrogen fixation in the western North Atlantic, Sci. Rep.-UK, 11, 5508, https://doi.org/10.1038/s41598-021-84969-1, 2021.

Wang, W. L., Moore, J. K., Martiny, A. C., and Primeau, F. W.: Convergent estimates of marine nitrogen fixation, Nature, 566, 205–213, https://doi.org/10.1038/s41586-019-0911-2, 2019.

Wannicke, N., Benavides, M., Dalsgaard, T., Dippner, J. W., Montoya, J. P., and Voss, M.: New perspectives on nitrogen Fixation measurements using ¹⁵N₂ Gas, Front. Marine Sci., 5, 120, https://doi.org/10.3389/fmars.2018.00120, 2018.

Wasmund, N., Struck, U., Hansen, A., Flohr, A., Nausch, G., Grüttmüller, A., and Voss, M.: Missing nitrogen fixation in the Benguela region, Deep-Sea Res. Pt. I, 106, 30–41, https://doi.org/10.1016/j.dsr.2015.10.007, 2015.

Watkins-Brandt, K., Letelier, R., Spitz, Y., Church, M., Böttjer, D., and White, A.: Addition of inorganic or organic phosphorus enhances nitrogen and carbon fixation in the oligotrophic North Pacific, Marine Ecol. Prog. Ser., 432, 17–29, https://doi.org/10.3354/meps09147, 2011.

Wen, Z., Lin, W., Shen, R., Hong, H., Kao, S.-J., and Shi, D.: Nitrogen fixation in two coastal upwelling regions of the Taiwan Strait, Sci. Rep.-UK, 7, 17601, https://doi.org/10.1038/s41598-017-18006-5, 2017.

Wen, Z., Browning, T. J., Cai, Y., Dai, R., Zhang, R., Du, C., Jiang, R., Lin, W., Liu, X., Cao, Z., Hong, H., Dai, M., and Shi, D.: Nutrient regulation of biological nitrogen fixation across the tropical western North Pacific, Sci. Adv., 8, eabl7564, https://doi.org/10.1126/sciadv.abl7564, 2022.

White, A. E., Watkins-Brandt, K. S., and Church, M. J.: Temporal variability of *Trichodesmium* spp. and diatom-diazotroph assemblages in the North Pacific Subtropical Gyre, Front. Mar. Sci., 5, 27, https://doi.org/10.3389/fmars.2018.00027, 2018.

White, A. E., Granger, J., Selden, C., Gradoville, M. R., Potts, L., Bourbonnais, A., Fulweiler, R. W., Knapp, A. N., Mohr, W., Moisander, P. H., Tobias, C. R., Caffin, M., Wilson, S. T., Benavides, M., Bonnet, S., Mulholland, M. R., and Chang, B. X.: A critical review of the ¹⁵N₂ tracer method to measure diazotrophic

production in pelagic ecosystems, Limnol. Oceanogr.-Methods, 18, 129–147, https://doi.org/10.1002/lom3.10353, 2020.

White, A. E., Granger, J., and Turk-Kubo, K.: Questioning high nitrogen fixation rate measurements in the Southern Ocean, Nat. Geosci., 15, 29–30, https://doi.org/10.1038/s41561-021-00873-3, 2022.

Wilson, S. T., Böttjer, D., Church, M. J., and Karl, D. M.: Comparative assessment of nitrogen fixation methodologies, conducted in the oligotrophic North Pacific Ocean, Appl. Environ. Microbiol., 78, 6516–6523, https://doi.org/10.1128/aem.01146-12, 2012.

Wilson, S. T., Aylward, F. O., Ribalet, F., Barone, B., Casey, J. R., Connell, P. E., Eppley, J. M., Ferrón, S., Fitzsimmons, J. N., Hayes, C. T., Romano, A. E., Turk-Kubo, K. A., Vislova, A., Armbrust, E. V., Caron, D. A., Church, M. J., Zehr, J. P., Karl, D. M., and DeLong, E. F.: Coordinated regulation of growth, activity and transcription in natural populations of the unicellular nitrogen-fixing cyanobacterium *Crocosphaera*, Nat. Microbiol., 2, 17118, https://doi.org/10.1038/nmicrobiol.2017.118, 2017.

Woebken, D., Burow, L. C., Behnam, F., Mayali, X., Schintlmeister, A., Fleming, E. D., Prufert-Bebout, L., Singer, S. W., Cortés, A. L., Hoehler, T. M., Pett-Ridge, J., Spormann, A. M., Wagner, M., Weber, P. K., and Bebout, B. M.: Revisiting N2 fixation in Guerrero Negro intertidal microbial mats with a functional single-cell approach, ISME J., 9, 485–496, https://doi.org/10.1038/ismej.2014.144, 2015.

Wu, C., Kan, J., Liu, H., Pujari, L., Guo, C., Wang, X., and Sun, J.: Heterotrophic bacteria dominate the diazotrophic community in the Eastern Indian Ocean (EIO) during pre-southwest monsoon, Microb. Ecol., 78, 804–819, https://doi.org/10.1007/s00248-019-01355-1, 2019.

Wu, C., Sun, J., Liu, H., Xu, W., Zhang, G., Lu, H., and Guo, Y.: Evidence of the significant contribution of heterotrophic diazotrophs to nitrogen fixation in the Eastern Indian Ocean during pre-southwest monsoon period, Ecosystems, 25, 1066–1083, https://doi.org/10.1007/s10021-021-00702-z, 2021.

Yeung, L. Y., Berelson, W. M., Young, E. D., Prokopenko, M. G., Rollins, N., Coles, V. J., Montoya, J. P., Carpenter, E. J., Steinberg, D. K., Foster, R. A., Capone, D. G., and Yager, P. L.: Impact of diatom-diazotroph associations on carbon export in the Amazon River plume, Geophys. Res. Lett., 39, L18609, https://doi.org/10.1029/2012GL053356, 2012.

Yogev, T., Rahav, E., Bar-Zeev, E., Man-Aharonovich, D., Stambler, N., Kress, N., Béjà, O., Mulholland, M. R., Herut, B., and Berman-Frank, I.: Is dinitrogen fixation significant in the Levantine Basin, East Mediterranean Sea?, Environ. Microbiol., 13, 854–871, https://doi.org/10.1111/j.1462-2920.2010.02402.x, 2011.

Zehr, J. P.: Nitrogen fixation by marine cyanobacteria, Trends Microbiol., 19, 162–173, https://doi.org/10.1016/j.tim.2010.12.004, 2011.

Zehr, J. P. and Capone, D. G.: Marine nitrogen fixation, Springer, https://doi.org/10.1007/978-3-030-67746-6, 2021.

Zehr, J. P. and Riemann, L.: Quantification of gene copy numbers is valuable in marine microbial ecology: A comment to Meiler et al. (2022), Limnol. Oceanogr., 68, 1406–1412, https://doi.org/10.1002/lno.12364, 2023.

Zhang, R., Chen, M., Yang, Q., Lin, Y., Mao, H., Qiu, Y., Tong, J., Lv, E., Yang, Z., Yang, W., and Cao, J.: Physical-biological coupling of N₂ fixation in the northwestern South China Sea coastal upwelling during summer, Limnol. Oceanogr., 60, 1411–1425, https://doi.org/10.1002/lno.10111, 2015.

Zhang, R., Zhang, D., Chen, M., Jiang, Z., Wang, C., Zheng, M., Qiu, Y., and Huang, J.: N₂ fixation rate and diazotroph community structure in the western tropical North Pacific Ocean, Acta Oceanol. Sin., 38, 26–34, https://doi.org/10.1007/s13131-019-1513-4, 2019.

Zhang, X., Ward, B. B., and Sigman, D. M.: Global nitrogen cycle: critical enzymes, organisms, and processes for nitrogen budgets and dynamics, Chem. Rev., 120, 5308–5351, https://doi.org/10.1021/acs.chemrev.9b00613, 2020.